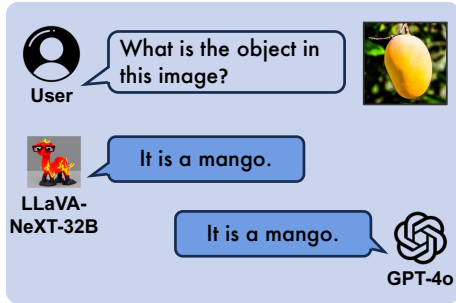


NEMO 🦒: Can Multimodal LLMs Identify Attribute-Modified Objects?

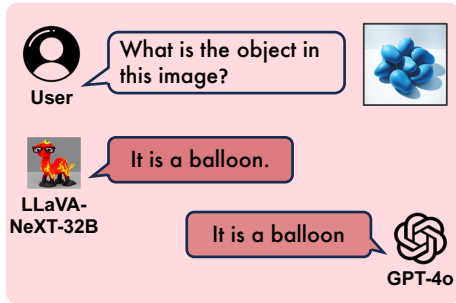
Jiaxuan Li¹, Junwen Mo¹, Duc Minh Vo¹, Akihiro Sugimoto², Hideki Nakayama¹

¹The University of Tokyo, Japan ²National Institute of Informatics, Japan

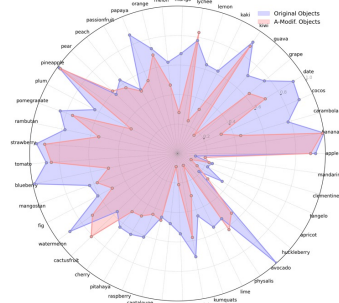
{li, mo, vmduc}@nlab.ci.i.u-tokyo.ac.jp sugimoto@nii.ac.jp nakayama@ci.i.u-tokyo.ac.jp



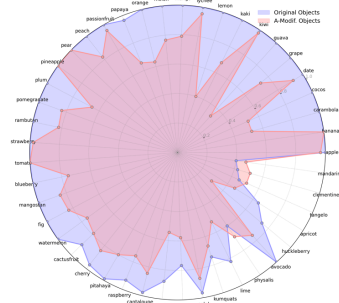
(a) Original Object



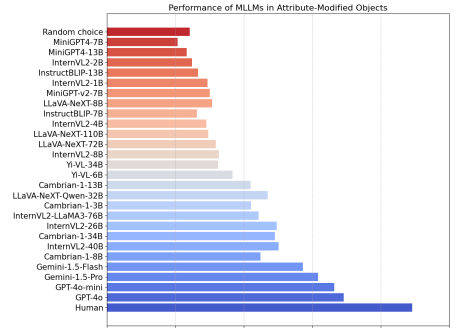
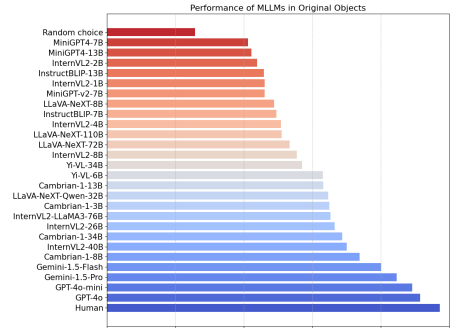
(b) Attribute-Modified Object



(c) LLaVA-NeXT-32B Performance



(d) GPT-4o Performance



(e) Results of Representative MLLMs

Figure 1. Challenges in consistently identifying original and attribute-modified objects are illustrated in (a) and (b): while LLaVA-NeXT-Qwen-32B and GPT-4o correctly recognize the original “mango”, both fail with a blue variant. Panels (c) and (d) show average accuracy scores of LLaVA-NeXT-Qwen-32B and GPT-4o across objects in our NEMO, comparing **original** and **attribute-modified** versions. (e) provides a comparative overview of average scores for representative MLLMs on original (upper) and attribute-modified (lower) objects.

Abstract

Multimodal Large Language Models (MLLMs) have made notable advances in visual understanding, yet their abilities to recognize objects modified by specific attributes remain an open question. To address this, we explore MLLMs’ reasoning capabilities in object recognition, ranging from commonsense to beyond-commonsense scenarios. We introduce a novel benchmark, NEMO¹, which comprises 900 images of original fruits and their corresponding attribute-modified ones; along with a set of 2,700 questions including open-, multiple-choice-, unsolvable types.

We assess 26 recent open-sourced and commercial models using our benchmark. The findings highlight pronounced performance gaps in recognizing objects in NEMO and reveal distinct answer preferences across different models. Although stronger vision encoders improve performance, MLLMs still lag behind standalone vision encoders. Interestingly, scaling up the model size does not consistently yield better outcomes, as deeper analysis reveals that larger LLMs can weaken vision encoders during fine-tuning. These insights shed light on critical limitations in current MLLMs and suggest potential pathways toward developing more versatile and resilient multimodal models.

¹Our NEMO and evaluation code are available at <https://jiaxuan-li.github.io/NEMO>.

1. Introduction

Our world is constantly changing, and with it comes the possibility of unexpected events - such as all mango skins suddenly turning blue (Fig. 1). With prior knowledge, humans would still recognize these “blue mango” despite the modified color. Yet, could MLLMs do the same when objects are modified by beyond-commonsense attributes? — This question is the motivation of this work.

Multimodal Large Language Models (MLLMs) [7, 14, 19, 23, 28, 34, 40, 46] have demonstrated remarkable capabilities in various visual understanding tasks, benefiting from the extensive world knowledge embedded within Large Language Models (LLMs) [2, 5, 36]. As MLLMs continue to evolve, a thorough exploration of their visual understanding and reasoning capabilities is essential, as it paves the way for developing more reliable and robust multimodal models. A wide range of benchmarks have been developed, focusing on basic perception tasks [13, 16, 17, 23], as well as more specialized challenges within commonsense, such as reasoning under adversarial conditions [18, 45, 47] and mitigating hallucination [15, 22, 38]. While prior studies have extensively addressed commonsense scenarios [4, 16, 17, 21, 42, 43], our work fully ventures into the area of MLLM behavior as it shifts from commonsense to beyond-commonsense reasoning. This is because, as we stated above, our world always changes and the beyond-commonsense “blue mango” resulting from mutation may come out. Developing MLLMs to handle such novel situations is crucial in advancing them to human-level AI [25, 27]. As a first step, this study aims to comprehensively assess existing MLLMs to answer our motivation question while giving insights for developing more versatile and resilient models.

We begin by evaluating MLLMs’ performance concerning the transition from recognizing **original objects** to **attribute-modified objects**, to understand how well they adapt when object attributes deviate from commonsense expectations. Focusing on beyond-commonsense reasoning is not entirely new: as summarized in Tab. 1, overarching objectives of a few benchmarks [3, 32, 48] are closely aligned with ours. However, attribute-modified object identification remains largely under-explored. These benchmarks do not provide sufficient insight into MLLMs’ capabilities when facing our scenario. Furthermore, they cannot be directly employed in our work due to the following reasons. (i) They lack a set of standard original objects for comparison. Standard original objects enable the model’s responses to be assessed based on how well it identifies the object when its attributes change. Without these reference objects, it becomes challenging to determine if the model consistently understands both the original object and its variant. (ii) Not all images in these benchmarks contain a single object with a clearly modified attribute, yet it is still identifiable for humans based on their prior knowledge and adaptable percep-

tion ability. This point is essential to evaluate the model effectively. (iii) None of them provide well-constructed VQA annotations to comprehensively test if the model can identify objects.

To address above limitations, we introduce NEMO, a benchmark designed to systematically evaluate MLLMs’ reasoning from commonsense to beyond-commonsense scenarios. NEMO includes 900 images and 2,700 carefully designed VQA annotations, covering 45 original objects and their attribute-modified counterparts. We choose fruits as our target objects due to their easily modifiable attributes and clear recognizability, addressing limitation (ii). Original objects are manually collected from the internet, while attribute-modified objects are generated by altering colors using DALL-E3 [30], addressing limitation (i). The VQA task in NEMO involves recognizing objects in open, multiple-choice, and unsolvable questions, testing MLLMs’ ability to identify objects via their own knowledge, choose between correct and deceptive options, and reject all deceptive choices, thereby addressing limitation (iii).

As illustrated in Fig. 1e, we evaluate a variety of open-sourced and commercial models, including GPT-4o [28] and Gemini-1.5-Pro [14], and conduct a user study to measure human performance. Our main contributions and findings can be summarized as follows:

- We provide NEMO, a new MLLM benchmark consisting of original objects and their attribute-modified counterparts, designed to fully assess the model from commonsense to beyond-commonsense. Note that we also extend NEMO to cover shape-modified fruits and color-modified animals (Sec. 5.4), which is further detailed in the Supplemental Material (SM).
- Extensive experiments on 26 MLLMs reveal significant performance gaps between original and attribute-modified object recognition, and between open-sourced and commercial MLLMs (Fig. 1c-e, more in Sec. 5.1).
- We analyze factors causing performance drop in MLLMs, providing insights for developing more robust MLLMs (Secs. 5.2 and 5.3): (1) MLLMs with stronger vision encoders perform better overall, but performance falls short of that achieved by their vision encoders alone. (2) Scaling model size does not consistently improve recognition of original or attribute-modified objects. (3) Stronger vision encoders benefit the recognition performance of MLLMs, while larger LLMs will weaken the vision encoders during fine-tuning. (4) MLLMs exhibit preferences in their responses for certain objects.

2. Related Work

Visual understanding benchmarks for MLLMs. They can be roughly categorized into general visual understanding and key capability evaluations (Tab. 1). (1) For the former, LLaVA-Bench [23], MME [13], MMBench [24] and SEED-Bench-1 [17] focus on basic perception, with

Table 1. Comparison of NEMO with recent visual understanding benchmarks for MLLMs, in terms of scale (VQA and image count), domain (real and synthetic), question type (yes/no, open, multiple-choice, and unsolvable questions), object type (fine-grained and attribute-modified), whether human or GPT is evaluated (H/G Eval.), evaluation objectives, and the number of evaluated models.

Benchmark	Scale		Domain		Question Type				Object Type		What to Evaluate	#Models	H/G Eval.
	#VQA	#Img.	Real	Synth.	Y/N	Open	Choice	Unsol.	Orig.	Attr.-Mod.			
General Visual Understanding Evaluation													
LLaVA-Bench [23]	60	24	✓			✓			✓		Basic perception	4	GPT
MME [13]	1,457	1,187	✓		✓				✓		Basic perception	6	GPT
MMBench [24]	3,217	3,217	✓						✓		Basic perception	14	GPT
SEED-Bench-1 [17]	19,242	–	✓						✓		Basic perception	18	N/A
SEED-Bench-2 [16]	24,371	–	✓						✓		Basic perception	23	N/A
MMMU [42]	11,500	–	✓			✓			✓		Expert-level domain knowledge	30	Human&GPT
MMMU-Pro [42]	3,460	–	✓			✓			✓		Expert-level domain knowledge	21	GPT
Key Capability Evaluation within Commonsense													
NaturalBench [18]	7,600	–	✓		✓				✓		Natural adversarial samples reasoning	53	Human&GPT
UPD [26]	2,095	–	✓					✓	✓		Answer withholding	7	GPT
FoodieQA [21]	403	389	✓						✓		Fine-grained food recognition	15	Human&GPT
MMVP [35]	300	300	✓		✓				✓		Visual perception for CLIP-blind pairs	8	Human&GPT
HaloQuest [38]	7,748	3,157	✓	✓		✓			✓		Hallucination mitigation	16	GPT
Visual Riddles [4]	400	400	✓	✓		✓			✓		Visual riddles requiring commonsense	6	Human&GPT
Reasoning beyond Commonsense													
ISEKAI [32]	–	1,498		✓					✓		Novel concept learning	5	N/A
WHOOPS [3]	3,374	500		✓		✓			✓		Abnormal element explanation	6	Human&GPT
ROME [48]	–	1,563		✓		✓			✓		Counter-intuitive content interpretation	6	N/A
NEMO (Ours)	2,700	900	✓	✓		✓	✓	✓	✓	✓	Attribute-modified object identification	26	Human&GPT

SEED-Bench-2 [16] supporting interleaved image-text input and image&text output, MMMU [42] and MMMU-Pro [43] requiring expert-level domain knowledge. (2) For the latter, specialized benchmarks test various abilities, including reasoning on natural adversarial samples (NaturalBench [18]), withholding answers (UPD [26]), fine-grained recognition of food (FoodieQA [21]), visual perception for CLIP-blind pairs (MMVP [35]), hallucination mitigation (HaloQuest [38]), and visual riddles using commonsense (Visual Riddles [4]). In contrast, NEMO aims to advance reasoning from commonsense to beyond commonsense.

Beyond-commonsense benchmarks for MLLMs. Recent benchmarks have emerged to evaluate MLLMs’ reasoning beyond commonsense. ISEKAI [32] creates unreal objects by transferring real-world objects into an “Isekai” world, testing whether models can learn novel concepts. WHOOPS [3] collects “weird” images with unusual object co-occurrences, assessing if models can explain abnormal elements. The most relevant work to NEMO is ROME [48], which generates counterintuitive images by modifying attributes and positional relations, to evaluates models on interpreting such content. However, our NEMO differs in several ways: (1) NEMO evaluates models’ ability to reason from commonsense to beyond commonsense by connecting attribute-modified objects in novel situations to their original counterparts in normal situations. (2) It provides both original objects and their attribute-modified versions for comprehensive evaluation. (3) Attribute-modified objects in NEMO are filtered out through human validation to ensure truly novel attributes unseen in the real world.

3. NEMO Benchmark

We here describe how we create NEMO. More detail can be found in SM.

3.1. Selection of Objects

As explained in Sec. 1, we mainly target fruits to build NEMO since they generally have simple structures and appearances, making it relatively easy to modify their colors. We select 45 common categories from Fruit360 dataset [37]. We note that we merge similar categories such as “*passion fruit*” and “*maracuja*” to “*passion fruit*” to lift potential ambiguities for MLLMs and even human. The full list of categories is in SM.

3.2. Data Collection

To examine MLLMs’ reasoning from commonsense to beyond commonsense, we collect images of both original and attribute-modified objects, with samples displayed in Fig. 2. **Original objects collection.** We collect ten images per category from the internet, resulting in 450 images of original fruits. Each image undergoes a manual check to ensure no additional objects are presented, maintaining dataset clarity. **Attribute-modified objects collection.** For each object, we generate ten attribute-modified images using DALL-E [30] with prompts like “*An image of {color} {object}*”, producing 450 images. The *color* refers to the novel color provided by GPT-4o [28], verified through manual inspection. We conduct manual checks and re-generation to ensure (1) The modified attributes are distinct from those in the original objects; (2) The attribute-modified objects remain recogniz-

Original	A-Modif.	Open Question	Multiple-Choice Question	Unsolvable Question
		Q: What is the object in this image? Please only reply with an object name. Correct Answer: Mango	Q: What is the object in this image? Please choose from the following 4 options: A: avocado, B: mango, C: apple, D: egg. Please only reply with the letter (A, B, C, or D). Correct Answer: B	Q: What is the object in this image? Please choose from the following 4 options: A: egg, B: apple, C: avocado, D: all other options are incorrect Please only reply with the letter (A, B, C, or D). Correct Answer: D
		Q: What is the object in this image? Please only reply with an object name. Correct Answer: Mangosteen	Q: What is the object in this image? Please choose from the following 4 options: A: pomegranate, B: tomato, C: mangosteen, D: apple. Please only reply with the letter (A, B, C, or D). Correct Answer: C	Q: What is the object in this image? Please choose from the following 4 options: A: apple, B: pomegranate, C: tomato, D: all other options are incorrect Please only reply with the letter (A, B, C, or D). Correct Answer: D
		Q: What is the object in this image? Please only reply with an object name. Correct Answer: Avocado	Q: What is the object in this image? Please choose from the following 4 options: A: egg, B: avocado, C: apple, D: pear. Please only reply with the letter (A, B, C, or D). Correct Answer: B	Q: What is the object in this image? Please choose from the following 4 options: A: egg, B: apple, C: pear, D: all other options are incorrect Please only reply with the letter (A, B, C, or D). Correct Answer: D

Figure 2. Samples from the NEMO benchmark, showcasing original and attribute-modified (A-Modif) objects with three types of question formats: open questions, multiple-choice questions, and unsolvable questions. We additionally circularly shift the choices 3 times in multiple-choice questions and unsolvable questions for extensive evaluation.

able to humans, meaning their categories are preserved.

3.3. QA Generation

We created three types of questions to assess MLLMs’ reasoning capability in original and attribute-modified objects:

Open question. This type of question asks the model to identify the object in the image without providing any options, relying solely on its own knowledge. As the open question examples shown in Fig. 2, the question is “*What is the object in this image? Please only reply with an object name.*” This format evaluates the model’s ability to provide direct, accurate responses.

Multiple-choice question. In these questions, we provide four possible options, including the correct answer and three distractors. The model is expected to select the correct answer by choosing the letter associated with the object name. As the multiple-choice question examples shown in Fig. 2, the question is like, “*What is the object in this image? Please choose from the following 4 options: A: {distractor₁}, B: {distractor₂}, C: {correct object}, D: {distractor₃}. Please only reply with the letter (A, B, C, or D).*” This format evaluates the model’s ability to differentiate between similar or related objects.

Unsolvable question. These questions are designed to test the model’s handling of unsolvable problems in the context of visual question answering [26]. In each case, four options are provided, but none of them has the candidate object correctly matching the object in the image. The model is expected to select the option indicating that all other choices are incorrect. As the unsolvable question examples shown in Fig. 2, it is in a format of, “*What is the object in this image? Please choose from the following 4 options: A: {distractor₁}, B: {distractor₂}, C: {distractor₃}, D: all other options are incorrect.*” This format evaluates the model’s ability to give a suitable response even when there are no correct objects in the options.

In sum, we have 2,700 (three for each image) questions.

4. Experimental Settings

Representative MLLM models. We evaluate a total of 26 MLLMs, including (1) **open-sourced models:** LLaVA-NeXT [19] (8B, 32B, 72B, 110B), InternVL2 [7] (1B, 2B, 4B, 8B, 26B, 40B, 76B), Cambrian-1 [34] (3B, 8B, 13B, 34B), Yi-VL [41] (6B, 34B), InstructBLIP [9] (7B, 13B), MiniGPT4 [49] (7B, 13B), MiniGPT-v2 [6] (7B); and (2) **commercial models:** GPT-4o [28], GPT-4o-mini [28], Gemini-1.5-Flash [14], Gemini-1.5-Pro [14]. We used the most up-to-date versions of each model, as of October 2024.

Circular shifting choice strategy. As suggested in [24], MLLMs might prefer to predict a certain choice among multiple choices. We employ a circular shifting choice strategy in multiple-choice and unsolvable questions, resulting in feeding the questions to MLLMs four (number of choices) times with circular shifting choices.

Model evaluation strategy. For most models, we extract a single word or option directly from the model’s output, or, if needed, parse the output to obtain a single word or option to compare with the ground truth. For models like Cambrian-1 [34] and MiniGPT4 [49], which often produce sentences, we employ GPT-4o [28] to evaluate the alignment between the model’s response and the ground truth. A question is considered correctly answered if the model’s output matches the ground truth. We use these results to compute accuracy scores. More details are in SM.

5. Experimental Results

5.1. Overall Comparison

Tab. 2 presents the evaluations on various MLLMs. Note that these MLLMs vary in vision encoders and LLMs.

Table 2. Performance in terms of accuracy (%) scores of 26 representative MLLMs on NEMO, including open-sourced and commercial models, human and random choice baselines. Higher score is better. Results cover original and attribute-modified objects, with performance gaps (Δ) between them for each question type. **Bold** marks the best results, and **original** marks the second best.

Method	Components		Original Objects				Attribute-Modified Objects							
	Vision Encoder	LLM	Open	Choice	Unsol.	Average	Open	Δ_O	Choice	Δ_C	Unsol.	Δ_U	Average	Δ_A
Baselines														
Human	-	-	96.6 \pm 3.6	98.7 \pm 0.6	98.8 \pm 0.5	98.0	87.3 \pm 7.5	-9.3	88.3 \pm 5.8	-10.4	91.8 \pm 6.6	-7.0	89.1	-8.9
Random choice	-	-	-	24.4 \pm 2.7	27.0 \pm 1.7	25.7	-	-	24.2 \pm 2.5	-0.2	24.1 \pm 2.0	-2.9	24.2	-1.5
Open-Sourced Models														
LLaVA-NeXT-8B [19]	CLIP-ViT-L-14-336	LLaMA3 _{8B}	42.0	77.2 \pm 0.8	27.1 \pm 13.9	48.8	24.9	-17.1	43.4 \pm 1.0	-33.8	23.8 \pm 14.2	-3.3	30.7	-18.1
LLaVA-NeXT-Qwen-32B [19]	SigLIP-ViT-SO-14-384	Qwen1.5 _{32B}	58.0	93.8 \pm 0.3	42.0 \pm 16.5	64.6	35.8	-22.2	72.0 \pm 1.0	-21.8	33.1 \pm 16.2	-8.9	47.0	-17.6
LLaVA-NeXT-72B [19]	CLIP-ViT-L-14-336	Qwen1.5 _{72B}	47.6	84.5 \pm 0.5	28.2 \pm 9.7	53.4	24.2	-23.4	49.4 \pm 0.8	-35.1	21.9 \pm 8.4	-6.3	31.8	-21.6
LLaVA-NeXT-110B [19]	CLIP-ViT-L-14-336	Qwen1.5 _{110B}	51.3	85.5 \pm 1.2	16.2 \pm 8.3	51.0	26.9	-24.4	52.2 \pm 0.6	-33.3	9.8 \pm 4.1	-6.4	29.6	-21.4
InternVL2-1B [7]	InternViT-300M-448	Qwen2-Instruct _{0.5B}	45.3	71.5 \pm 1.0	21.6 \pm 10.4	46.1	24.0	-21.3	50.2 \pm 2.4	-21.3	13.9 \pm 4.6	-7.7	29.4	-16.7
InternVL2-2B [7]	InternViT-300M-448	InternLM2-Chat _{1.8B}	49.6	68.4 \pm 0.5	13.8 \pm 0.4	43.9	25.6	-24.0	40.4 \pm 0.8	-28.0	8.4 \pm 1.5	-5.4	24.8	-19.1
InternVL2-4B [7]	InternViT-300M-448	Phi3-Mini-128K-Instruct _{3.8B}	50.9	82.9 \pm 0.7	18.6 \pm 6.0	50.8	23.3	-27.6	52.7 \pm 0.7	-30.2	11.2 \pm 2.5	-7.4	29.1	-21.7
InternVL2-8B [7]	InternViT-300M-448	InternLM2.5-Chat _{7B}	50.7	84.3 \pm 0.5	31.3 \pm 5.2	55.4	25.8	-24.9	50.2 \pm 1.7	-34.1	22.0 \pm 8.5	-9.3	32.7	-22.7
InternVL2-26B [7]	InternViT-6B-448-V1.5	InternLM2-Chat _{20B}	79.3	96.0 \pm 0.5	24.3 \pm 8.1	66.5	53.3	-26.0	80.6 \pm 0.6	-15.4	15.0 \pm 6.8	-9.3	49.6	-16.9
InternVL2-40B [7]	InternViT-6B-448-V1.5	Nous-Hermes2-Yi _{32B}	69.6	95.4 \pm 0.3	44.9 \pm 8.6	70.0	41.3	-28.3	73.5 \pm 1.0	-21.9	35.5 \pm 11.0	-9.4	50.1	-19.9
InternVL2-LLaMA3-76B [7]	InternViT-6B-448-V1.5	Hermes2-Theta-LLaMA3 _{70B}	73.3	87.0 \pm 0.9	35.7 \pm 6.1	65.3	44.4	-28.9	63.4 \pm 0.5	-23.6	25.0 \pm 6.2	-10.7	44.3	-21.0
Cambrian-1-3B [34]	SigLIP-ViT-SO-14	Phi3 _{3.8B}	58.9	91.8 \pm 0.4	44.4 \pm 3.6	65.0	32.4	-26.5	71.1 \pm 0.7	-20.7	22.7 \pm 4.7	-21.7	42.1	-22.9
Cambrian-1-8B [34]	+CLIP-ViT-L-14	LLaMA3 _{8B}	62.9	91.8 \pm 0.5	66.8 \pm 3.7	73.8	36.7	-26.2	67.4 \pm 1.6	-24.4	30.3 \pm 4.5	-36.5	44.8	-29.0
Cambrian-1-13B [34]	+DINOv2-g	Vicuna1.5 _{13B}	59.8	88.0 \pm 1.4	41.7 \pm 3.4	63.2	37.1	-22.7	65.5 \pm 1.1	-22.5	23.5 \pm 3.5	-18.2	42.0	-21.2
Cambrian-1-34B [34]	+CLIP-ConvNeXT-XXL	Hermes2-Yi _{34B}	65.3	92.8 \pm 0.1	48.1 \pm 5.3	68.7	55.6	-9.7	66.4 \pm 1.1	-26.4	24.9 \pm 2.8	-23.2	49.0	-19.7
Yi-VL-6B [41]	CLIP-ViT-H-14-224	Yi-Chat _{6B}	57.6	87.8 \pm 0.9	44.0 \pm 10.4	63.1	30.4	-27.2	55.5 \pm 1.1	-32.3	24.2 \pm 7.1	-19.8	36.7	-26.4
Yi-VL-34B [41]	CLIP-ViT-H-14-224	Yi-Chat _{34B}	53.6	91.2 \pm 1.6	26.3 \pm 11.2	57.0	25.8	-27.8	52.7 \pm 1.5	-38.5	19.1 \pm 9.5	-7.2	32.5	-24.5
InstructBLIP-7B [9]	EVA01-ViT-G-14-224	Vicuna _{7B}	72.9	57.3 \pm 12.6	18.2 \pm 29.5	49.5	23.3	-49.6	44.3 \pm 10.1	-13.0	11.2 \pm 14.5	-7.0	26.3	-23.2
InstructBLIP-13B [9]	EVA01-ViT-G-14-224	Vicuna _{13B}	68.0	59.1 \pm 14.4	10.2 \pm 9.3	45.8	31.6	-36.4	41.6 \pm 9.3	-17.5	6.5 \pm 7.9	-3.7	26.6	-19.2
MiniGPT4-7B [49]	EVA01-ViT-G-14-224	Vicuna _{7B}	54.9	53.8 \pm 1.7	14.8 \pm 3.6	41.2	30.9	-24.0	22.4 \pm 3.5	-31.4	8.7 \pm 4.2	-6.1	20.7	-20.5
MiniGPT4-13B [49]	EVA01-ViT-G-14-224	Vicuna _{13B}	54.9	66.4 \pm 2.5	5.2 \pm 1.7	42.2	31.3	-23.6	31.4 \pm 1.3	-35.0	7.3 \pm 2.9	+2.1	23.3	-18.9
MiniGPT-v2-7B [6]	EVA01-ViT-G-14-224	LLaMA2 _{7B}	51.6	65.1 \pm 4.7	21.7 \pm 27.1	46.1	26.0	-25.6	47.3 \pm 4.3	-17.8	16.7 \pm 23.3	-5.0	30.0	-16.1
Commercial Models														
GPT-4o [28]	-	-	90.9	99.3 \pm 0.2	84.2 \pm 1.9	91.5	56.2	-34.7	77.6 \pm 1.0	-21.7	73.4 \pm 7.5	-10.8	69.1	-22.4
GPT-4o-mini [28]	-	-	85.3	95.4 \pm 0.4	87.0 \pm 1.1	89.2	49.6	-35.7	72.0 \pm 0.9	-23.4	77.7 \pm 2.4	-9.3	66.4	-22.8
Gemini-1.5-Flash [14]	-	-	86.2	96.1 \pm 1.2	57.9 \pm 15.0	80.1	63.3	-22.9	79.2 \pm 0.9	-16.9	29.2 \pm 10.5	-28.7	57.2	-22.9
Gemini-1.5-Pro [14]	-	-	86.4	99.2 \pm 0.4	68.3 \pm 1.0	84.6	62.2	-24.2	83.6 \pm 1.5	-15.6	39.1 \pm 8.8	-29.2	61.6	-23.0

Human evaluation confirms the quality of NEMO. We engage human annotators to answer questions in random order, as detailed in SM. Human performance serves as the baseline in this comparison, achieving consistently high scores across all question types for both original and attribute-modified objects. This high performance reflects the reliability and quality of the constructed dataset, providing a solid foundation for evaluating MLLMs on commonsense and beyond-commonsense reasoning.

MLLMs’ performance declines on objects with modified attributes. Across all models, there is a noticeable performance drop when moving from original to attribute-modified objects. This trend highlights the challenge MLLMs face in recognizing objects with modified attributes, requiring beyond-commonsense reasoning. For example, Cambrian-1-8B [34] achieves an average score of 73.8 on original objects but drops to 44.8 on attribute-modified objects. Even GPT-4o [28], exhibits a significant decline of 22.4, revealing a general limitation in handling attribute modifications effectively.

When examining the three question types, the performance drop is most pronounced in open and multiple-choice questions when shifting from original to attribute-modified objects. For unsolvable questions, both open-sourced and certain commercial models, such as Gemini [14], perform poorly on original and attribute-modified objects with high standard deviations. This variability in-

dicates instability and inconsistency in MLLMs’ responses when choices are circularly shifted in unsolvable questions. **Open-sourced MLLMs underperform compared to commercial models, especially on attribute-modified objects.** Commercial models, such as GPT-4o [28] and GPT-4o-mini [28], lead in performance across both original and attribute-modified objects, with GPT-4o reaching a top average of 91.5 on original objects and 69.1 on attribute-modified objects. In contrast, open-sourced MLLMs, like Cambrian-1-8B [34] and InternVL2-40B [7], generally score lower, with averages of 73.8 on original objects and 50.1 on attribute-modified objects, respectively.

Furthermore, the performance gap between commercial and open-sourced MLLMs widens further on attribute-modified objects. For example, the gap between GPT-4o [28] and Cambrian-1-8B [34] is 17.7 on original objects, while it becomes 24.3 on attribute-modified objects.

Overall, these results indicate current MLLMs, even GPT-4o [28], need substantial improvements to handle beyond-commonsense reasoning effectively. Therefore, we explore performance decline within the MLLM architecture in Sec. 5.2, model preferences for certain objects within NEMO in Sec. 5.3, and samples outside NEMO in Sec. 5.4, to offer deeper insights into this problem.

5.2. Probing Performance Drop within Model Itself

In this section, we examine the reasons behind the performance drop observed when open-sourced MLLMs en-

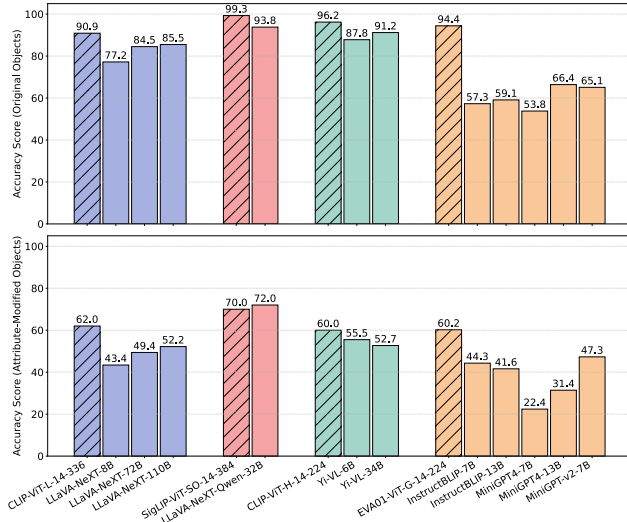


Figure 3. Model accuracy scores across vision encoders for multiple-choice questions on original objects (upper) and attribute-modified objects (lower). MLLMs using the same vision encoder are shown in the same color, while vision encoders themselves are distinguished by diagonal line patterns. Stronger encoders generally improve MLLM performance, yet most MLLMs perform worse than their encoders.

counter attribute-modified objects from the aspects of model components and model sizes.

Question 1: How does the pre-trained vision encoder in MLLMs contribute to the performance gap?

We compare the model performance in original objects (Fig. 3, upper) and attribute-modified objects (Fig. 3, lower), focusing on the different vision encoders used in MLLM models, including CLIP-ViT-L-14-336 [29], SigLIP-ViT-SO-14-384 [44], CLIP-ViT-H-14-224 [29], and EVA01-ViT-G-14-224 [31]. Note here the results for the vision encoder come from the pre-trained vision encoder. To get accuracy scores for vision encoders, we compare the image embeddings from the vision encoder, with the text embeddings generated by corresponding text encoder for object names in the multiple-choice questions. So, for fair comparison, the results of MLLMs presented here are from the multiple-choice accuracy score.

As shown in Fig. 3 upper, if pre-trained vision encoders perform better, MLLMs with the same vision encoder also generally perform well on original objects. Specifically, models with encoders such as SigLIP-ViT-SO-14-384 [44] and CLIP-ViT-H-14-224 [29] demonstrate high accuracy across different MLLMs. However, a surprising finding is that, across most models, a single pre-trained vision encoder consistently outperforms the MLLMs that use it. This discrepancy suggests that the current MLLMs’ vision-language alignment might be a limiting factor, as the projector and LLM fail to fully leverage the robust embeddings provided by high-performance pre-trained vision encoders.

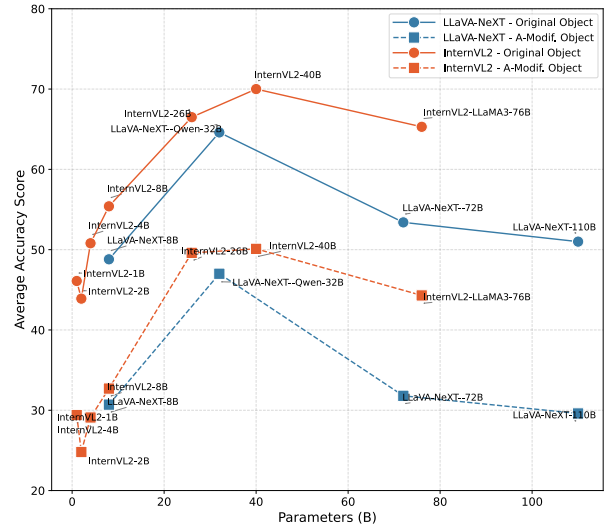


Figure 4. Average accuracy scores of various MLLMs (LLaVA-NeXT and InternVL2 series) for all question types across different model sizes on original and attribute-modified objects. The performance does not consistently improve as the model size increases.

A similar pattern emerges in the results on attribute-modified objects, as seen in Fig. 3 lower. Interestingly, LLaVA-NeXT-Qwen-32B [19], utilizing the SigLIP-ViT-SO-14-384 [44] vision encoder, demonstrates a notable exception by achieving a slightly higher accuracy on attribute-modified objects than the standalone performance of its vision encoder. This suggests that being equipped with enough strong vision encoders may help mitigate some of the performance losses on modified attributes.

Answer 1: While advanced vision encoders contribute to improved recognition in original and modified objects, the full potential of these encoders is not fully realized in current MLLM models. Addressing this performance gap will likely require innovations in integrating vision and language components more effectively.

Question 2: How does MLLM size affect the gap?

We analyze average scores of MLLMs for all question types with varying model sizes, including LLaVA-NeXT [19] (8B to 110B) and InternVL2 [7] (1B to 76B), on both original and attribute-modified objects, as shown in Fig. 4.

For both original and attribute-modified objects, increasing the model size generally leads to improved performance initially. Smaller models such as InternVL2-1B and LLaVA-NeXT-8B show relatively low accuracy on both object types, while accuracy improves with models like InternVL2-26B and LLaVA-NeXT-Qwen-32B, suggesting MLLMs benefit from more parameters.

However, as model size continues to increase, we observe a decline in accuracy, particularly on attribute-modified objects. For example, from LLaVA-NeXT-Qwen-32B to LLaVA-NeXT-72B, performance decreases by 15.2 on attribute-modified objects and by 11.2 on original ob-

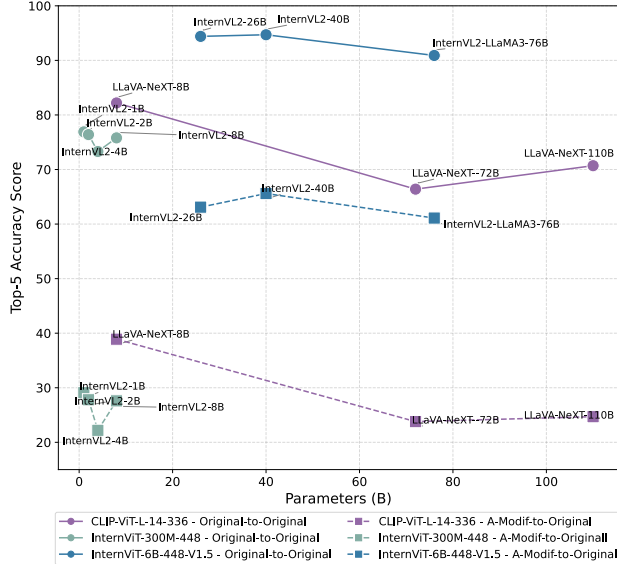


Figure 5. Top-5 accuracy of Original-to-Original and Attribute-modified-to-Original object matching, using image representations obtained from MLLMs’ trained vision encoders. Fine-tuning with larger LLMs may weaken the vision encoders.

jects. This indicate that, beyond a certain size, additional parameters may add complexity that hinders the model’s adaptation to modified attributes.

Answer 2: Simply scaling up model size does not guarantee better handling of attribute modifications. Future research should consider optimizing model architectures and training techniques specifically to address the challenges posed by attribute-modified objects, rather than relying solely on increased model size.

Question 3: Why does scaling up MLLM size not guarantee better performance?

To answer this question, we separate vision encoders and LLMs in MLLMs to analyze how scaling up each component affects performance. Unlike *Question 1*, which focuses on pretrained vision encoders, we separate the vision encoder from the whole MLLMs after fine-tuning; then evaluate its image representation. We employ image-to-image matching for this experiment including Original-to-Original (O2O) and Attribute-modified-to-Original (A2O) matching. For each query, a matching is considered correct if one of the top five similar images belongs to the same category (details in SM).

Fig. 5 shows that fine-tuning the same pre-trained vision encoder with different LLMs in MLLMs yields varied performance. Vision encoders fine-tuned on InternViT-300M-448 perform similarly, possibly because their small scale MLLM limits further improvement. In contrast, larger MLLMs like LLaVA-NeXT-72B and LLaVA-NeXT-110B, perform worse than LLaVA-NeXT-8B. A similar, al-

beit less pronounced, trend is observed for InternVL2-26B, InternVL2-40B, and InternVL2-LLaMA3-76B, suggesting that fine-tuning with larger LLMs may weaken the vision encoder’s performance. As noted in *Question 2*, LLaVA-NeXT-8B achieves comparable performance to LLaVA-NeXT-72B and LLaVA-NeXT-110B on attribute-modified objects, despite significantly larger scales of the latter two.

Answer 3: Stronger vision encoders improve MLLM performance, but larger LLMs often weaken vision encoders during fine-tuning. Preserving vision encoder strength is essential, especially when fine-tuning with larger LLMs.

5.3. Exploring Model Preferences in NEMO

Question 4: Do MLLMs prefer certain objects?

In Fig 6, we compare model performance on both original and attribute-modified objects, grouped by object categories. This analysis provides insights into how different MLLMs perform across objects and if certain categories are easier or more challenging for the models to recognize.

Overall, for original objects, MLLMs perform best on common and easily recognizable objects, such as “apple”, “avocado”, and “banana”. These objects, due to their familiarity and distinctive features, seem to pose fewer challenges for models. However, performance declines significantly for less common or visually complex objects, such as “clementine”, “huckleberry”, and “salak”. The degradation is amplified when applied to objects with modified attributes, suggesting rare or less familiar objects are especially challenging for MLLMs to recognize accurately when presented with modified attributes.

Answer 4: MLLMs show a preference for certain objects, particularly those that are common and easily recognizable. In contrast, they struggle with less common objects, especially when objects are presented with modified attributes. This suggests that while MLLMs are effective at recognizing frequently encountered items, they face significant challenges in generalizing to rare or atypical objects, particularly when those objects have non-standard appearances.

5.4. Investigating outside NEMO

In this section, we briefly discuss the results on our NEMO-extension which consists of shape-modified fruits and color-modified animals. Refer to SM for more details.

Question 5: How do MLLMs perform on objects with other modified attributes rather than colors?

In addition to color modifications, we explore the performance of MLLMs on objects with other attribute changes by generating shape-modified images. Using DALL-E [30], we generate images with prompts in the format, “An image of {shape} {object}”, which resulted in a collection of 450 images with modified shapes, ultimately yielding 260 shape-modified images after selection.

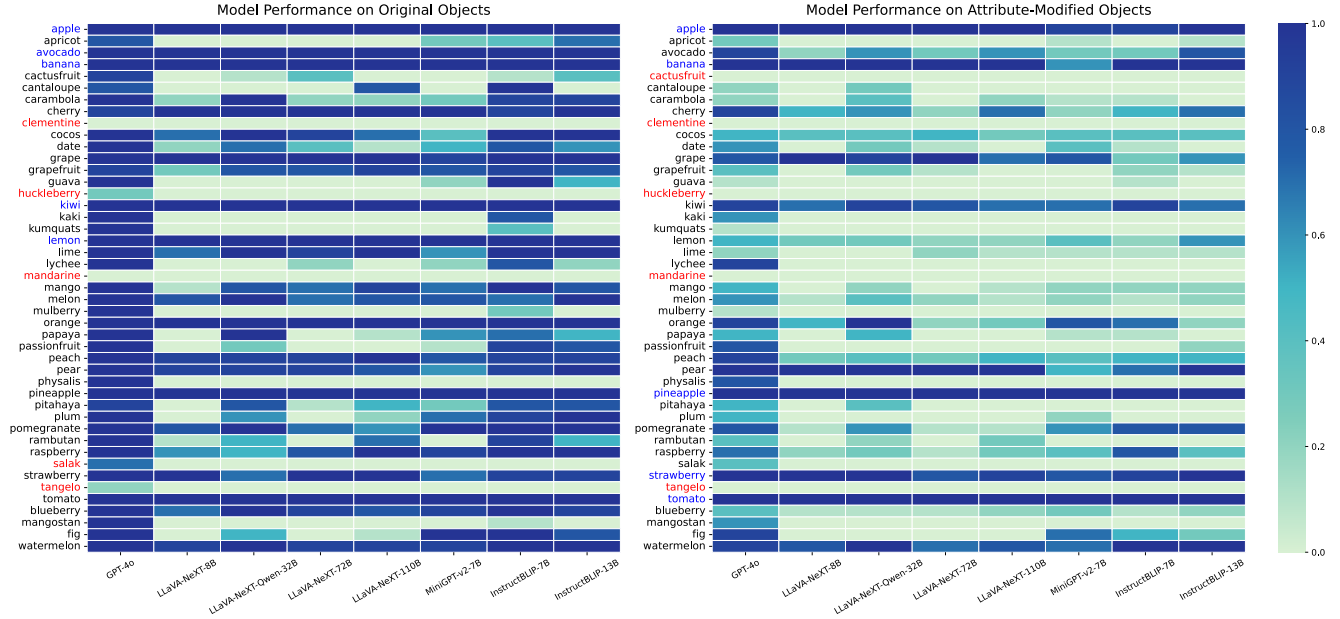


Figure 6. Comparison of model performance on different fruits in original objects (left) and attribute-modified objects (right) for open questions. Each heatmap illustrates the accuracy of various models (x-axis) when applied to different fruit types (y-axis), with dark blue indicating higher performance and light green indicating lower performance. Top-5 object names which all MLLMs prefer most and least are highlighted in blue and red, respectively.

The results of MLLMs on objects with modified shapes are provided in SM, showing a performance pattern similar to that observed on color-modified objects (Tab. 2).

Answer 5: MLLMs face comparable challenges when recognizing objects with non-standard shapes as they do with color alterations. This consistency suggests that the difficulties MLLMs encounter are not solely tied to specific types of attribute modifications but rather to any deviation from typical object appearances.

Question 6: How do MLLMs perform on other objects rather than fruits?

To extend our analysis beyond fruits, we select 42 animal categories from ImageNet [10]. The generation process for attribute-modified images follows a similar approach, using prompts in the format, “An image of {animal} with {color} skin, replacing its usual skin”. After filtering, we get 218 images of animals with modified attributes.

Our SM shows the results. Consistent with prior findings, MLLMs show a decline in recognition performance on objects with modified attributes. Additionally, open-sourced MLLMs continue to underperform compared to commercial models like GPT-4o and Gemini-1.5-Pro, both on original and attribute-modified animal objects.

Answer 6: MLLMs exhibit similar performance trends on non-fruit objects as on fruits. This further demonstrates the limitations of MLLMs in generalizing to attribute-modified representations across various object types, not just fruits.

6. Discussion and Limitations

First, a primary limitation in using generated data for model evaluation is the lack of diversity [11], which can influence the visual characteristics of generated images. We will explore methods to mitigate these biases in generated data, such as use well-designed prompts to increase the diversity. Second, while this study focuses primarily on object recognition as a component of semantic reasoning in visual understanding, effective object understanding requires a broader range of skills, including spatial reasoning and contextual interpretation. Future research should aim to evaluate MLLMs across a wider range of visual tasks to better understand their limitations in consistently interpreting both original and attribute-modified objects.

7. Conclusion

To answer “Could MLLMs identify objects when they are modified by beyond-commonsense attributes?”, we propose NEMO to evaluate 26 MLLMs’ performance on both original and attribute-modified objects, revealing that while MLLMs excel with common objects, their accuracy drops notably for objects with modified attributes. Open-sourced models, in particular, lag behind commercial models like GPT-4o. Key factors contributing to this gap include vision encoder choice, training processes, and model size, with MLLMs struggling to fully utilize strong vision encoders. We believe that using NEMO as a testbed could lay out potential roadmaps to enhance versatile and resilient MLLMs.

References

- [1] Jean-Baptiste Alayrac, Jeff Donahue, Pauline Luc, Antoine Miech, Iain Barr, Yana Hasson, Karel Lenc, Arthur Mensch, Katherine Millican, Malcolm Reynolds, et al. Flamingo: A visual language model for few-shot learning. In *Advances in Neural Information Processing Systems (NeurIPS)*, 2022. 12
- [2] Jinze Bai, Shuai Bai, Yunfei Chu, Zeyu Cui, Kai Dang, Xiaodong Deng, Yang Fan, Wenbin Ge, Yu Han, Fei Huang, Binyuan Hui, Luo Ji, Mei Li, Junyang Lin, Runji Lin, Dayiheng Liu, Gao Liu, Chengqiang Lu, Keming Lu, Jianxin Ma, Rui Men, Xingzhang Ren, Xuancheng Ren, Chuanqi Tan, Sinan Tan, Jianhong Tu, Peng Wang, Shijie Wang, Wei Wang, Shengguang Wu, Benfeng Xu, Jin Xu, An Yang, Hao Yang, Jian Yang, Shusheng Yang, Yang Yao, Bowen Yu, Hongyi Yuan, Zheng Yuan, Jianwei Zhang, Xingxuan Zhang, Yichang Zhang, Zhenru Zhang, Chang Zhou, Jingren Zhou, Xiaohuan Zhou, and Tianhang Zhu. Qwen technical report. *arXiv preprint arXiv:2309.16609*, 2023. 2, 12
- [3] Nitzan Bitton-Guetta, Yonatan Bitton, Jack Hessel, Ludwig Schmidt, Yuval Elovici, Gabriel Stanovsky, and Roy Schwartz. Breaking common sense: WHOOPS! A vision-and-language benchmark of synthetic and compositional images. In *Proc. IEEE/CVF International Conference on Computer Vision (ICCV)*, 2023. 2, 3
- [4] Nitzan Bitton-Guetta, Aviv Slobodkin, Aviya Maimon, Eliya Habba, Royi Rassin, Yonatan Bitton, Idan Szepkter, Amir Globerson, and Yuval Elovici. Visual riddles: A common-sense and world knowledge challenge for large vision and language models. *arXiv preprint arXiv:2407.19474*, 2024. 2, 3
- [5] Zheng Cai, Maosong Cao, Haojiong Chen, Kai Chen, Keyu Chen, Xin Chen, Xun Chen, Zehui Chen, Zhi Chen, Pei Chu, Xiaoyi Dong, Haodong Duan, Qi Fan, Zhaoye Fei, Yang Gao, Jiaye Ge, Chenya Gu, Yuzhe Gu, Tao Gui, Aijia Guo, Qipeng Guo, Conghui He, Yingfan Hu, Ting Huang, Tao Jiang, Penglong Jiao, Zhenjiang Jin, Zhikai Lei, Jiaying Li, Jingwen Li, Linyang Li, Shuaibin Li, Wei Li, Yining Li, Hongwei Liu, Jiangning Liu, Jiawei Hong, Kaiwen Liu, Kuikun Liu, Xiaoran Liu, Chengqi Lv, Haijun Lv, Kai Lv, Li Ma, Runyuan Ma, Zerun Ma, Wenchang Ning, Linke Ouyang, Jiantao Qiu, Yuan Qu, Fukai Shang, Yunfan Shao, Demin Song, Zifan Song, Zhihao Sui, Peng Sun, Yu Sun, Huanze Tang, Bin Wang, Guoteng Wang, Jiaqi Wang, Jiayu Wang, Rui Wang, Yudong Wang, Ziyi Wang, Xingjian Wei, Qizhen Weng, Fan Wu, Yingtong Xiong, Chao Xu, Ruiliang Xu, Hang Yan, Yirong Yan, Xiaogui Yang, Haochen Ye, Huaiyuan Ying, Jia Yu, Jing Yu, Yuhang Zang, Chuyu Zhang, Li Zhang, Pan Zhang, Peng Zhang, Ruijie Zhang, Shuo Zhang, Songyang Zhang, Wenjian Zhang, Wenwei Zhang, Xingcheng Zhang, Xinyue Zhang, Hui Zhao, Qian Zhao, Xiaomeng Zhao, Fengzhe Zhou, Zaida Zhou, Jingming Zhuo, Yicheng Zou, Xipeng Qiu, Yu Qiao, and Dahua Lin. InternLM2 technical report. *arXiv preprint arXiv:2403.17297*, 2024. 2, 12
- [6] Jun Chen, Deyao Zhu, Xiaoqian Shen, Xiang Li, Zechu Liu, Pengchuan Zhang, Raghuraman Krishnamoorthi, Vikas Chandra, Yunyang Xiong, and Mohamed Elhoseiny. MiniGPT-v2: Large language model as a unified interface for vision-language multi-task learning. *arXiv preprint arXiv:2310.09478*, 2023. 4, 5, 12, 13, 19
- [7] Zhe Chen, Weiyun Wang, Hao Tian, Shenglong Ye, Zhangwei Gao, Erfei Cui, Wenwen Tong, Kongzhi Hu, Jiapeng Luo, Zheng Ma, et al. How far are we to GPT-4V? Closing the gap to commercial multimodal models with open-source suites. *arXiv preprint arXiv:2404.16821*, 2024. 2, 4, 5, 6, 12, 19, 20
- [8] Wei-Lin Chiang, Zhuohan Li, Zi Lin, Ying Sheng, Zhanghao Wu, Hao Zhang, Lianmin Zheng, Siyuan Zhuang, Yonghao Zhuang, Joseph E. Gonzalez, Ion Stoica, and Eric P. Xing. Vicuna: An open-source chatbot impressing GPT-4 with 90%* ChatGPT quality, 2023. 12
- [9] Wenliang Dai, Junnan Li, Dongxu Li, Anthony Tiong, Junqi Zhao, Weisheng Wang, Boyang Li, Pascale Fung, and Steven Hoi. InstructBLIP: Towards general-purpose vision-language models with instruction tuning. In *Advances in Neural Information Processing Systems (NeurIPS)*, 2023. 4, 5, 12, 13, 19
- [10] Jia Deng, Wei Dong, Richard Socher, Li-Jia Li, Kai Li, and Li Fei-Fei. ImageNet: A large-scale hierarchical image database. In *Proc. IEEE/CVF Conference on Computer Vision and Pattern Recognition (CVPR)*, 2009. 8, 16
- [11] Lijie Fan, Kaifeng Chen, Dilip Krishnan, Dina Katabi, Phillip Isola, and Yonglong Tian. Scaling laws of synthetic images for model training ... for now. In *Proc. IEEE/CVF Conference on Computer Vision and Pattern Recognition (CVPR)*, 2024. 8
- [12] Yuxin Fang, Wen Wang, Binhui Xie, Quan Sun, Ledell Wu, Xinggang Wang, Tiejun Huang, Xinlong Wang, and Yue Cao. EVA: Exploring the limits of masked visual representation learning at scale. In *Proc. IEEE/CVF Conference on Computer Vision and Pattern Recognition (CVPR)*, 2023. 12
- [13] Chaoyou Fu, Peixian Chen, Yunhang Shen, Yulei Qin, Mengdan Zhang, Xu Lin, Jinrui Yang, Xiawu Zheng, Ke Li, Xing Sun, et al. MME: A comprehensive evaluation benchmark for multimodal large language models. *arXiv preprint arXiv:2306.13394*, 2023. 2, 3
- [14] Google. Gemini., 2023. 2, 4, 5, 19, 20
- [15] Tianrui Guan, Fuxiao Liu, Xiyang Wu, Ruiqi Xian, Zongxia Li, Xiaoyu Liu, Xijun Wang, Lichang Chen, Furong Huang, Yaser Yacoob, Dinesh Manocha, and Tianyi Zhou. HallusionBench: An advanced diagnostic suite for entangled language hallucination and visual illusion in large vision-language models. In *Proc. IEEE/CVF Conference on Computer Vision and Pattern Recognition (CVPR)*, 2024. 2
- [16] Bohao Li, Yuying Ge, Yixiao Ge, Guangzhi Wang, Rui Wang, Ruimao Zhang, and Ying Shan. SEED-Bench-2: Benchmarking multimodal large language models. *arXiv preprint arXiv:2311.17092*, 2023. 2, 3
- [17] Bohao Li, Yuying Ge, Yixiao Ge, Guangzhi Wang, Rui Wang, Ruimao Zhang, and Ying Shan. SEED-Bench: Benchmarking multimodal large language models. In *Proc. IEEE/CVF Conference on Computer Vision and Pattern Recognition (CVPR)*, 2024. 2, 3
- [18] Baiqi Li, Zhiqiu Lin, Wenxuan Peng, Jean de Dieu Nyandwi, Daniel Jiang, Zixian Ma, Simran Khanuja, Ranjay Krishna,

- Graham Neubig, and Deva Ramanan. Naturalbench: Evaluating vision-language models on natural adversarial samples. In *Neural Information Processing Systems (NeurIPS) Datasets and Benchmarks Track*, 2024. 2, 3
- [19] Bo Li, Kaichen Zhang, Hao Zhang, Dong Guo, Renrui Zhang, Feng Li, Yuanhan Zhang, Ziwei Liu, and Chunyuan Li. LLaVA-NeXT: Stronger LLMs supercharge multimodal capabilities in the wild, 2024. 2, 4, 5, 6, 12, 19, 20
- [20] Junnan Li, Dongxu Li, Silvio Savarese, and Steven Hoi. BLIP-2: Bootstrapping language-image pre-training with frozen image encoders and large language models. In *Proc. International Conference on Machine Learning (ICML)*, 2023. 12
- [21] Wenyan Li, Xinyu Zhang, Jiaang Li, Qiwei Peng, Raphael Tang, Li Zhou, Weijia Zhang, Guimin Hu, Yifei Yuan, Anders Søgaard, et al. FoodieQA: A multimodal dataset for fine-grained understanding of chinese food culture. *Proc. Conference on Empirical Methods in Natural Language Processing (EMNLP)*, 2024. 2, 3
- [22] Yifan Li, Yifan Du, Kun Zhou, Jinpeng Wang, Xin Zhao, and Ji-Rong Wen. Evaluating object hallucination in large vision-language models. In *Proc. Conference on Empirical Methods in Natural Language Processing (EMNLP)*, 2023. 2
- [23] Haotian Liu, Chunyuan Li, Qingyang Wu, and Yong Jae Lee. Visual instruction tuning. In *Advances in Neural Information Processing Systems (NeurIPS)*, 2023. 2, 3, 12
- [24] Yuan Liu, Haodong Duan, Yuanhan Zhang, Bo Li, Songyang Zhang, Wangbo Zhao, Yike Yuan, Jiaqi Wang, Conghui He, Ziwei Liu, et al. MMBench: Is your multi-modal model an all-around player? In *Proc. European Conference on Computer Vision (ECCV)*, 2024. 2, 3, 4
- [25] John McCarthy. From here to human-level AI. *Artificial Intelligence*, 171(18):1174–1182, 2007. 2
- [26] Atsuyuki Miyai, Jingkan Yang, Jingyang Zhang, Yifei Ming, Qing Yu, Go Irie, Yixuan Li, Hai Li, Ziwei Liu, and Kiyoharu Aizawa. Unsolvable problem detection: Evaluating trustworthiness of vision language models. *arXiv preprint arXiv:2403.20331*, 2024. 3, 4
- [27] Meredith Ringel Morris, Jascha Sohl-Dickstein, Noah Fiedel, Tris Warkentin, Allan Dafoe, Aleksandra Faust, Clement Farabet, and Shane Legg. Position: Levels of AGI for operationalizing progress on the path to AGI. In *Proc. International Conference on Machine Learning (ICML)*, 2024. 2
- [28] OpenAI. GPT-4o, 2024. 2, 3, 4, 5, 12, 13, 19, 20
- [29] Alec Radford, Jong Wook Kim, Chris Hallacy, Aditya Ramesh, Gabriel Goh, Sandhini Agarwal, Girish Sastry, Amanda Askell, Pamela Mishkin, Jack Clark, et al. Learning transferable visual models from natural language supervision. In *Proc. International Conference on Machine Learning (ICML)*, 2021. 6, 12
- [30] Aditya Ramesh, Mikhail Pavlov, Gabriel Goh, Scott Gray, Chelsea Voss, Alec Radford, Mark Chen, and Ilya Sutskever. Zero-shot text-to-image generation. In *Proc. International Conference on Machine Learning (ICML)*, 2021. 2, 3, 7, 12, 16, 17
- [31] Quan Sun, Yuxin Fang, Ledell Wu, Xinlong Wang, and Yue Cao. EVA-CLIP: Improved training techniques for CLIP at scale. *arXiv preprint arXiv:2303.15389*, 2023. 6
- [32] Yan Tai, Weichen Fan, Zhao Zhang, and Ziwei Liu. Link-context learning for multimodal LLMs. In *Proc. IEEE/CVF Conference on Computer Vision and Pattern Recognition (CVPR)*, 2024. 2, 3
- [33] Maxim Tkachenko, Mikhail Malyuk, Andrey Holmanyuk, and Nikolai Liubimov. Label Studio: Data labeling software, 2020-2022. Open source software available from <https://github.com/heartexlabs/label-studio>. 13
- [34] Shengbang Tong, Ellis Brown, Penghao Wu, Sanghyun Woo, Manoj Middepogu, Sai Charitha Akula, Jihan Yang, Shusheng Yang, Adithya Iyer, Xichen Pan, Austin Wang, Rob Fergus, Yann LeCun, and Saining Xie. Cambrian-1: A fully open, vision-centric exploration of multimodal LLMs. In *Advances in Neural Information Processing Systems (NeurIPS)*, 2024. 2, 4, 5, 12, 13, 19
- [35] Shengbang Tong, Zhuang Liu, Yuexiang Zhai, Yi Ma, Yann LeCun, and Saining Xie. Eyes wide shut? Exploring the visual shortcomings of multimodal LLMs. In *Proc. IEEE/CVF Conference on Computer Vision and Pattern Recognition (CVPR)*, 2024. 3
- [36] Hugo Touvron, Thibaut Lavril, Gautier Izacard, Xavier Martinet, Marie-Anne Lachaux, Timothée Lacroix, Baptiste Rozière, Naman Goyal, Eric Hambro, Faisal Azhar, et al. LLaMA: Open and efficient foundation language models. *arXiv preprint arXiv:2302.13971*, 2023. 2, 12
- [37] Chiagoziem C Ukwuoma, Qin Zhiguang, Md Belal Bin Heyat, Liaqat Ali, Zahra Almaspoor, and Happy N Monday. Recent advancements in fruit detection and classification using deep learning techniques. *Mathematical Problems in Engineering*, 2022(1):9210947, 2022. 3
- [38] Zhecan Wang, Garrett Bingham, Adams Wei Yu, Quoc V. Le, Thang Luong, and Golnaz Ghiasi. HaloQuest: A visual hallucination dataset for advancing multimodal reasoning. In *Proc. European Conference on Computer Vision (ECCV)*, 2024. 2, 3
- [39] Le Xue, Manli Shu, Anas Awadalla, Jun Wang, An Yan, Senthil Purushwalkam, Honglu Zhou, Viraj Prabhu, Yutong Dai, Michael S Ryoo, Shrikant Kendre, Jieyu Zhang, Can Qin, Shu Zhang, Chia-Chih Chen, Ning Yu, Juntao Tan, Tulika Manoj Awalgaoonkar, Shelby Heinecke, Huan Wang, Yejin Choi, Ludwig Schmidt, Zeyuan Chen, Silvio Savarese, Juan Carlos Niebles, Caiming Xiong, and Ran Xu. xGen-MM (formerly BLIP-3): A family of open large multimodal models. *arXiv preprint arXiv:2408.08872*, 2024. 12
- [40] Qinghao Ye, Haiyang Xu, Guohai Xu, Jiabo Ye, Ming Yan, Yiyang Zhou, Junyang Wang, Anwen Hu, Pengcheng Shi, Yaya Shi, Chaoya Jiang, Chenliang Li, Yuanhong Xu, Hehong Chen, Junfeng Tian, Qian Qi, Ji Zhang, and Fei Huang. mPLUG-Owl: Modularization empowers large language models with multimodality. *arXiv preprint arXiv:2304.14178*, 2023. 2
- [41] Alex Young, Bei Chen, Chao Li, Chengen Huang, Ge Zhang, Guanwei Zhang, Heng Li, Jiangcheng Zhu, Jianqun Chen, Jing Chang, et al. Yi: Open foundation models by 01. ai. *arXiv preprint arXiv:2403.04652*, 2024. 4, 5, 12, 19

- [42] Xiang Yue, Yuansheng Ni, Kai Zhang, Tianyu Zheng, Ruoqi Liu, Ge Zhang, Samuel Stevens, Dongfu Jiang, Weiming Ren, Yuxuan Sun, Cong Wei, Botao Yu, Ruibin Yuan, Renliang Sun, Ming Yin, Boyuan Zheng, Zhenzhu Yang, Yibo Liu, Wenhao Huang, Huan Sun, Yu Su, and Wenhua Chen. MMMU: A massive multi-discipline multimodal understanding and reasoning benchmark for Expert AGI. In *Proc. IEEE/CVF Conference on Computer Vision and Pattern Recognition (CVPR)*, 2024. 2, 3
- [43] Xiang Yue, Tianyu Zheng, Yuansheng Ni, Yubo Wang, Kai Zhang, Shengbang Tong, Yuxuan Sun, Botao Yu, Ge Zhang, Huan Sun, Yu Su, Wenhua Chen, and Graham Neubig. MMMU-Pro: A more robust multi-discipline multimodal understanding benchmark. *arXiv preprint arXiv:2409.02813*, 2024. 2, 3
- [44] Xiaohua Zhai, Basil Mustafa, Alexander Kolesnikov, and Lucas Beyer. Sigmoid loss for language image pre-training. In *Proc. IEEE/CVF International Conference on Computer Vision (ICCV)*, 2023. 6, 12
- [45] Hao Zhang, Wenqi Shao, Hong Liu, Yongqiang Ma, Ping Luo, Yu Qiao, and Kaipeng Zhang. AVIBench: Towards evaluating the robustness of large vision-language model on adversarial visual-instructions. *arXiv preprint arXiv:2403.09346*, 2024. 2
- [46] Pan Zhang, Xiaoyi Dong, Yuhang Zang, Yuhang Cao, Rui Qian, Lin Chen, Qipeng Guo, Haodong Duan, Bin Wang, Linke Ouyang, Songyang Zhang, Wenwei Zhang, Yining Li, Yang Gao, Peng Sun, Xinyue Zhang, Wei Li, Jingwen Li, Wenhao Wang, Hang Yan, Conghui He, Xingcheng Zhang, Kai Chen, Jifeng Dai, Yu Qiao, Dahua Lin, and Jiaqi Wang. InternLM-XComposer-2.5: A versatile large vision language model supporting long-contextual input and output. *arXiv preprint arXiv:2407.03320*, 2024. 2
- [47] Yunqing Zhao, Tianyu Pang, Chao Du, Xiao Yang, Chongxuan Li, Ngai-Man Cheung, and Min Lin. On evaluating adversarial robustness of large vision-language models. In *Advances in Neural Information Processing Systems (NeurIPS)*, 2023. 2
- [48] Kankan Zhou, Eason Lai, Wei Bin Au Yeong, Kyriakos Mouratidis, and Jing Jiang. ROME: Evaluating pre-trained vision-language models on reasoning beyond visual common sense. In *Findings of the Association for Computational Linguistics: EMNLP*, 2023. 2, 3
- [49] Deyao Zhu, Jun Chen, Xiaoqian Shen, Xiang Li, and Mohamed Elhoseiny. MiniGPT-4: Enhancing vision-language understanding with advanced large language models. In *International Conference on Learning Representations (ICLR)*, 2024. 4, 5, 12, 13, 19

Supplementary Material for NEMO 🦉: Can Multimodal LLMs Identify Attribute-Modified Objects?

This supplementary material complements our paper with the following sections:

- We discuss further related work on multimodal large language models (MLLMs) (see Sec. A), which were not covered in the main paper Sec. 2.
- A detailed description of the methodology used to construct our proposed NEMO benchmark is provided (see Sec. B).
- We elaborate on the experimental setup and methods used to assess model performance (see Sec. C).
- We provide analysis on failure cases observed in the results of MLLMs on NEMO (see Sec. D).
- We include additional evaluations of MLLMs on NEMO-extension including shape-modified fruits and color-modified animals, as well as NEMO with synthetic original objects and different open question prompts (see Sec. E).
- We discuss further considerations and observations related to this work (see Sec. F).

A. More Related Work

Multimodal large language models. Recent open-sourced MLLMs, such as LLaVA-NeXT [19], Yi-VL [41], InternVL2 [7], Cambrian-1 [34], and xGen-MM-base-4B (BLIP-3) [39] have been demonstrated strong capabilities in various visual-centric tasks. These models typically consist of three components: (1) a visual encoder, like CLIP vision encoder [12, 29, 44], which processes visual inputs; (2) a pre-trained large language model, such as Vicuna [8], LLaMA [36], Qwen [2], and InternLM [5], to handle multimodal embeddings and perform reasoning; and (3) a visual-language projector, such as cross-attention layers [1], MLPs [19, 23], a single linear layer [6, 49], and Q-Former [9, 20], to align the visual and language modalities. Given the diversity of MLLMs, evaluating them effectively is a critical challenge.

B. More Details about NEMO

B.1. Full List of Categories

The full list of 45 categories included in our NEMO is presented in the “*Object*” column of Tab. A.

B.2. Original Data Source

Image links of original data. The images of original objects are collected from the Internet (Fig. A). Due to copyright considerations, we will only provide the image links for original objects in our public NEMO.

B.3. Attribute-Modified Data Construction

Full list of modified attributes. The modified color refers to the novel color provided by GPT-4o [28] (Tab. A). These modifications are manually verified to ensure quality and accuracy.

Image generation. We utilize the OpenAI’s DALL-E3 [30] API with the model name of “dall-e-3”, size of “1024×1024”, quality of “standard”, to generate attribute-modified images.

B.4. Questions Construction

Multiple choices. To construct distractor choices for the multiple-choice questions and unsolvable questions, We collect misclassified objects from the open questions’s responses by GPT-4o [28], LLaVA-NeXT-8B [19], InstructBLIP-7B [9], InstructBLIP-13B [9], and MiniGPT-v2-7B [6]. We select Top-3 most frequent misclassified objects as the distractor options. For the objects with less than 3 misclassified objects, we manually add the distractor options after asking GPT-4o [28] to give some suggestions by prompts like “*Could you provide a list of objects that are often mistaken for {object} due to their similar appearance, color, or shape?*” The distractor options for each object are detailed in Tab. B.

B.5. Data Examples

Examples of original objects and attribute-modified objects are shown in Figs. A and B, respectively. All images in NEMO are standardized to a resolution of 1024×1024.

C. More Details on Model Evaluation

C.1. Evaluation Settings

For commercial models, we conduct experiments using CPU resources. For open-sourced models, we utilize a single RTX A6000 GPU (for models smaller than 26B) or multiple ones (for models larger than or equivalent to 26B) to evaluate models.

C.2. Human Evaluation Details

Human annotators. We recruit two annotators to volunteer in our human evaluation process.

Human evaluation manual. We design three types of questions for evaluating original objects and attribute-modified objects. Ideally, each annotator would handle only one question type to ensure every image is evaluated once. However, due to limited numbers of annotators, both annotators evaluated all question types. To minimize potential

Table A. All objects and the modified colors for each object in NEMO.

Object	Color ₁	Color ₂	Color ₃	Color ₄	Color ₅	Color ₆	Color ₇	Color ₈	Color ₉	Color ₁₀
apple	bright yellow	vibrant orange	rich purple	deep cyan	light green	sky blue	soft green	soft tangerine	light pink	blush pink
apricot	bright yellow	deep purple	vibrant green	lemon yellow	crimson red	soft pink	warm brown	deep cyan	sky blue	bright blue
avocado	soft pink	bright yellow	bright red	vibrant orange	light green	crimson red	golden	rich purple	bright cyan	blush pink
banana	bright red	deep purple	vibrant orange	light green	soft pink	vibrant pink	light green	deep red	rich blue	vidid red
blueberry	soft pink	bright yellow	light purple	deep red	vibrant orange	light green	warm brown	golden	vidid pink	bright red
cactusfruit	vibrant pink	deep red	bright red	warm brown	soft pink	lemon yellow	rich purple	bright red	bright yellow	vidid red
cantaloupe	bright blue	deep purple	golden	bright red	soft pink	light green	vidid red	vibrant orange	vidid pink	vibrant red
carambola	bright red	soft pink	bright blue	deep purple	deep orange	deep red	warm brown	sky blue	deep cyan	deep green
cherry	bright yellow	vibrant green	soft pink	vibrant orange	deep purple	vibrant green	light yellow	warm brown	bright cyan	deep blue
clementine	bright purple	deep purple	bright red	soft pink	vibrant green	deep red	bright blue	bright red	light green	vidid pink
cocos	soft pink	light green	bright red	vibrant orange	bright yellow	golden	rich purple	deep red	vibrant green	blush pink
date	bright yellow	soft pink	deep purple	bright red	light green	vibrant orange	warm brown	deep red	vidid pink	golden
fig	golden	soft pink	bright yellow	rich purple	deep red	vibrant orange	light blue	warm brown	vidid pink	bright red
grape	soft pink	rich cyan	deep red	vibrant orange	light cyan	warm brown	vidid pink	golden	bright blue	bright yellow
grapefruit	rich purple	bright yellow	soft pink	deep red	vibrant orange	light green	warm brown	golden	vidid pink	bright red
guava	bright yellow	rich purple	soft pink	deep red	vibrant orange	light green	warm brown	golden	vidid pink	bright red
huckleberry	soft pink	bright yellow	deep red	rich purple	vibrant orange	light green	vibrant blue	golden	vidid pink	bright red
kaki	soft pink	bright blue	rich purple	deep red	light green	vibrant cyan	warm brown	golden	bright red	vidid pink
kiwi	bright yellow	soft pink	rich purple	deep red	bright blue	light purple	deep cyan	bright blue	vidid pink	bright red
kumquats	soft pink	rich purple	deep red	vibrant blue	light green	warm brown	bright purple	vidid pink	bright red	bright blue
lemon	soft pink	rich purple	bright purple	deep red	vibrant orange	light green	warm brown	golden	vidid pink	bright red
lime	soft pink	bright blue	rich purple	bright cyan	vibrant blue	light pink	light red	bright red	vidid pink	bright red
lychee	bright yellow	rich purple	golden	soft pink	deep red	vibrant orange	light green	sky blue	bright red	vidid pink
mandarine	rich purple	bright blue	soft pink	deep red	vibrant cyan	light green	warm purple	sky blue	vidid pink	bright red
mango	soft pink	deep red	rich purple	bright blue	vibrant orange	light green	warm brown	golden	vidid pink	bright red
mangostan	soft pink	bright yellow	rich blue	deep red	vibrant orange	light green	bright cyan	golden	vidid pink	bright red
melon	bright purple	soft pink	black	deep red	bright cyan	light green	bright magenta	golden	vidid pink	bright red
mulberry	soft pink	bright yellow	rich purple	light pink	vibrant orange	light green	warm brown	golden	turquoise	vidid pink
orange	soft pink	light purple	deep red	vibrant turquoise	light green	light cyan	violet	vidid pink	sky blue	bright magenta
papaya	soft pink	bright yellow	rich purple	deep red	vibrant turquoise	light green	light purple	golden	vidid pink	bright red
passionfruit	bright yellow	soft pink	rich purple	bright cyan	vibrant orange	sky blue	golden	vidid pink	light green	bright red
peach	vibrant turquoise	soft purple	bright yellow	rich purple	deep red	vibrant orange	light green	sky blue	golden	bright cyan
pear	bright yellow	soft pink	rich purple	deep red	vibrant orange	light green	warm brown	golden	vidid pink	bright red
physalis	soft pink	bright yellow	rich purple	deep red	vibrant orange	light green	warm brown	golden	sky blue	bright red
pineapple	soft pink	sky blue	rich purple	deep red	vibrant orange	light green	vidid pink	warm brown	golden	bright red
pitahaya	bright yellow	sky blue	rich purple	soft purple	vibrant orange	light green	vibrant turquoise	golden	vibrant green	bright cyan
plum	soft pink	bright yellow	rich purple	deep red	light green	warm brown	golden	vidid pink	bright cyan	vibrant orange
pomegranate	soft pink	bright yellow	deep cyan	vibrant orange	rich purple	light green	warm brown	golden	bright blue	vidid pink
rambutan	soft pink	bright yellow	rich purple	sky blue	warm brown	vibrant orange	light green	golden	vidid pink	bright blue
raspberry	golden	bright yellow	soft pink	rich purple	deep blue	vibrant orange	light green	warm brown	bright cyan	bright purple
salak	soft pink	bright yellow	rich purple	deep red	vibrant orange	light green	warm brown	golden	vidid pink	bright red
strawberry	bright yellow	soft pink	rich purple	deep cyan	vibrant orange	light green	warm brown	golden	vidid pink	bright blue
tangelo	soft pink	bright blue	rich purple	deep red	vibrant cyan	turquoise	light green	warm purple	vidid pink	bright red
tomato	soft pink	bright yellow	rich purple	deep cyan	vibrant orange	light green	warm brown	golden	vidid pink	bright blue
watermelon	soft pink	bright yellow	rich purple	deep red	vibrant orange	light blue	warm brown	golden	vidid pink	bright red

evaluation bias, the order of image and question pairs is randomized, and these pairs are not revisited by the annotators during the evaluation process.

Human evaluation interface. An example of the human evaluation interface is shown in Fig. C. The interface is implemented using Label Studio [33].

C.3. Model Response Extraction

As described in main paper Sec. 4, for most models, we extract a single word or option directly from the model’s output. When necessary, we parse the output to obtain a comparable word or option. Singular, plural forms, and synonyms of object names are also considered.

While for models including InstructBLIP [9] (7B, 13B), MiniGPT4 [49] (7B, 13B), MiniGPT-v2-7B [6], and Cambrian-1 [34] (3B, 8B, 13B, 34B), which often produce sentences, we employ GPT-4o [28] assess alignment between the model’s response and the correct answer using the following prompt:

Prompt to Evaluate Model Responses via GPT-4o

```
Evaluate the following model response
based on the question and correct
answer:
Question: {question}
Correct Answer: {correct answer}
Model Response: {model response}
Is the model response correct? Please
reply with "Correct" or "Incorrect".
```

A question is marked correct if the model’s response matches the correct answer.

C.4. Image-to-Image Matching

In main paper Sec. 5.2 *Question 3*, we employ image-to-image matching to investigate “*Why does scaling up MLLM size not guarantee better performance?*” Here, we provide additional details on the image-to-image matching process.

To obtain the representation of each image, we compute

Table B. Distractor options for each object in the multiple-choice and unsolvable questions of NEMO.

Object	Distractor ₁	Distractor ₂	Distractor ₃
apple	orange	tomato	peach
apricot	ball	plum	peach
avocado	egg	pear	apple
banana	apple	orange	papaya
cactusfruit	tomato	berry	egg
cantaloupe	apple	watermelon	orange
carambola	star	flower	starfish
cherry	apple	bowl	orange
clementine	orange	apple	lemon
cocos	ball	onion	apple
date	pear	pomegranate	apple
grape	raspberry	ball	apple
grapefruit	orange	apple	ball
guava	apple	pumpkin	lemon
huckleberry	pomegranate	blueberry	bunch
kiwi	apple	tomato	orange
kaki	tomato	apple	pumpkin
kumquats	tomato	egg	orange
lemon	orange	ball	lime
lime	lemon	orange	ball
lychee	apple	strawberry	raspberry
mandarine	apple	tomato	orange
mango	egg	apple	avocado
melon	ball	pumpkin	apple
mulberry	raspberry	berry	grape
orange	apple	ball	lemon
papaya	banana	pumpkin	pear
passionfruit	pomegranate	orange	ball
peach	apple	quince	tomato
pear	apple	orange	strawberry
physalis	apple	tomato	berry
pineapple	apple	plum	strawberry
pitahaya	cactus	pineapple	artichoke
plum	apple	orange	apricot
pomegranate	apple	pumpkin	pear
rambutan	ball	cactu	mushroom
raspberry	apple	grape	blackberry
salak	orange	egg	pineapple
strawberry	blueberry	apple	orange
tangelo	orange	apple	lemon
tomato	apple	kaki	cherry
blueberry	apple	orange	ball
mangostan	apple	pomegranate	tomato
fig	onion	tomato	pomegranate
watermelon	pumpkin	ball	apple



Figure A. Sample for each original object in NEMO.

the average embedding of all tokens within the image, as MLLMs omit the [CLS] token. The representations of the original objects form the index set. For each query image, we calculate the cosine similarity between the query and the indexed images to identify the Top-5 most similar images.

In the Original-to-Original matching evaluation, we exclude the query image from the retrieved results to avoid trivial matches and ensure an unbiased evaluation.



Figure B. Sample for each attribute-modified object in NEMO.

D. Model Failures

D.1. Failure Cases for Open Questions

We present examples of failure cases for MLLMs when answering open questions in Figs. D to F, and identify several

failure patterns as follows:

Hallucinations from spurious correlations. MLLMs often produce hallucinated responses due to spurious correlations between visual features. For instance, in Fig. D, a “rich purple guava” with a shape resembling a pumpkin is frequently misclassified as “pumpkin” by most models. Similar issues occur in Fig. E and Fig. F: A “deep red kumquat” is misidentified as a “tomato” due to color similarity. A “vivid pink mandarin” is mistaken for an “apple” because of similar coloration, as well. We further analyze such hallucinations in multiple-choice question settings in Sec. D.2.

Vague responses. Some MLLMs like Gemini-1.5-Flash in Fig. D, InternVL2-8B, -40B, -LLaMA3-76B in Fig. E, and LLaVA-NeXT-110B, InstructBLIP-7B, MiniGPT-v2-7B in Fig. F, fail to provide a specific object name when uncertain. Instead, they respond with general terms like “fruit,” which do not meet the requirement for precise object identification. To address this, we design other question types including multiple-choice and unsolvable questions in the main paper, and also evaluate MLLMs with alternative open-question prompts in Sec. E.3.

Failure to interpret instructions. Some models fail to adhere to instruction prompts that specify concise responses. For example, models like InstructBLIP (7B, 13B), MiniGPT4 (7B, 13B), MiniGPT-v2-7B, and Cambrian-1 (3B, 8B, 13B, 34B) often generate full sentences instead of replying with a single object name. This behavior suggests these models struggle to interpret the instruction: “What is the object in this image? Please only reply with an object name.” To address this issue, we utilize GPT-4o to evaluate the alignment between these model outputs and correct answers, as described in Sec. C.3.

D.2. Hallucinations in Multiple-Choice Questions

In Fig. G, we visualize the results of LLaVA-NeXT-8B and its pre-trained vision encoder, CLIP-ViT-L-14-336, for multiple-choice questions on attribute-modified objects using chord diagrams. In the diagrams: the source node represents the correct object name. The target node represents the predicted object name. The edge color originates from the source node, indicating that the edge is linked from the correct object name to the predicted one. From the chord diagrams, we observe the following:

Increased Hallucinations in LLaVA-NeXT-8B. LLaVA-NeXT-8B exhibits significantly more hallucinations compared to its pre-trained vision encoder, CLIP-ViT-L-14-336. This observation further reinforces the conclusion from the main paper Sec. 5.2 *Question 1* that the full potential of these encoders has yet to be fully realized in current MLLM models.

Frequent misclassification as common and easily recognizable objects like “apple”. A considerable number of objects are incorrectly classified as “apple,” suggesting a potential bias in the model towards common and easily rec-

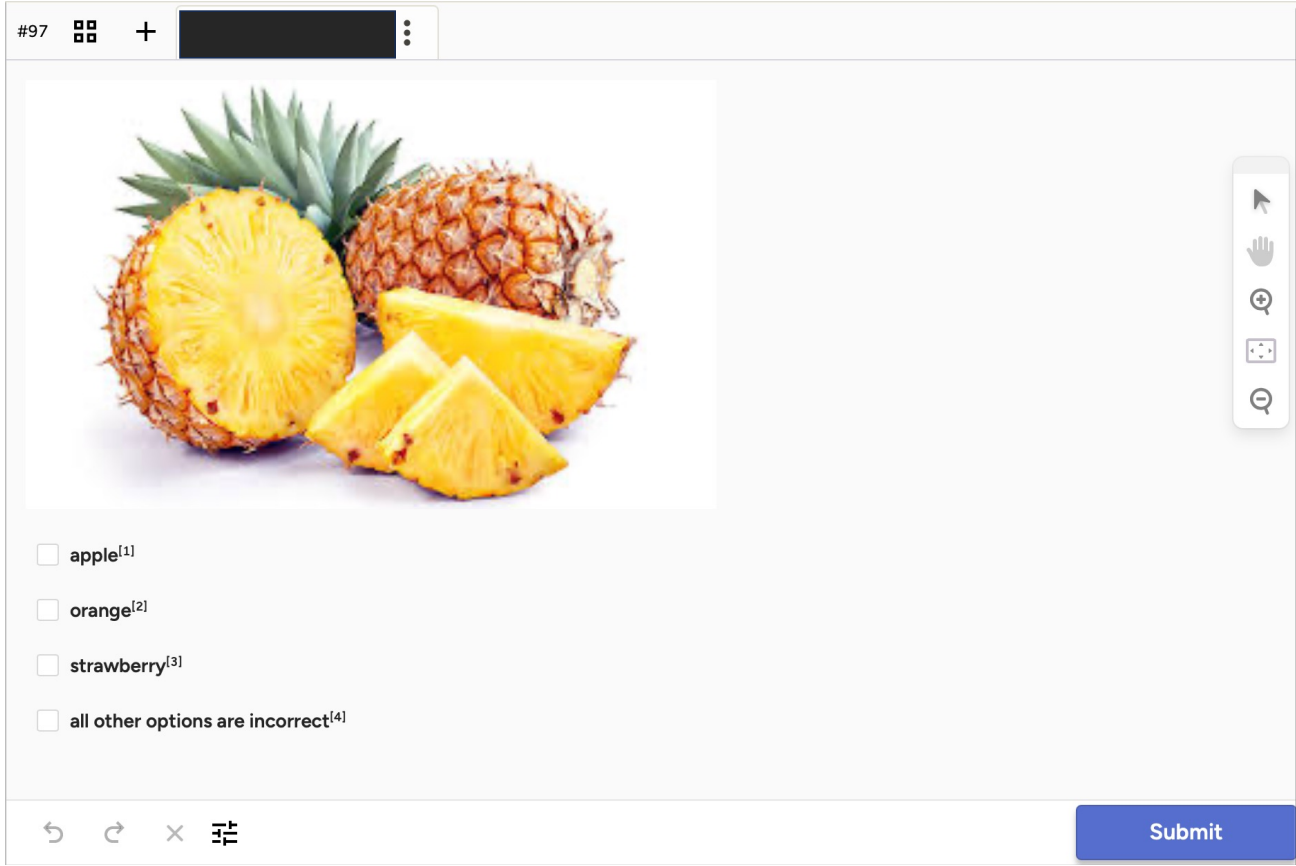


Figure C. Example of human evaluation interface.

ognizable objects.

These findings indicate that current MLLMs may introduce more hallucinations, especially for some and easily recognizable objects, during the fine-tuning process.

E. Further Analysis

E.1. Investigating on NEMO-Extension

In main paper Sec. 5.4 *Question 5* and *Question 6*, we discuss the findings obtained from experiments on our NEMO-extension, which includes datasets of shape-modified fruits and color-modified animals. Below, we elaborate on experimental details and results.

Collection of shape-modified fruits. In addition to color modifications, we explored the performance of MLLMs on objects with other attribute changes by generating shape-modified images. Using DALL-E [30], we generated images with prompts in the format, “*An image of {shape} {object}*”, which resulted in a collection of 450 images with modified shapes, ultimately yielding 260 shape-modified images after selection. We show some examples in Fig. H, and the modified shapes for each object in Tab. C.

Collection of original animals and color-modified ani-

mals. To extend our analysis beyond fruits, we select 42 animal categories from ImageNet [10]. The generation process for attribute-modified images follows a similar approach in our main paper, using prompts in the format, “*An image of {animal} with {color} skin, replacing its usual skin*”. After filtering, we get 218 images of animals with modified colors. The modified colors for each animal are shown in Tab. D.

To maintain consistency, we collected 218 original animal images from the Internet, matching the proportions of each animal category in the color-modified dataset. Examples of original and color-modified animals are presented in Fig. I and Fig. J, respectively.

Results on NEMO-extension Tab. E presents the results of MLLMs on objects with modified shapes. Note that, to compare fairly on the same data scale, the results for original fruits are reported as weighted averages derived from the main paper Sec. 5.1. These weights are calculated based on the proportion of each object category (e.g., “*apple*”) relative to the total number of objects in the shape-modified fruit dataset.

The performance pattern observed here aligns closely with that seen for color-modified fruits in NEMO, demon-

Table C. The modified shapes for each fruit in NEMO-extension.

Object	Shape ₁	Shape ₂	Shape ₃	Shape ₄	Shape ₅	Shape ₆	Shape ₇	Shape ₈	Shape ₉	Shape ₁₀
apple	triangle	hexagon	rectangle	pentagon	square	donut	cylinder	heart		
apricot	square	triangle	hexagon	pentagon	heart					
avocado	hexagon	star	cylinder							
banana	square	triangle	donut	pentagon	heart	hexagon	star	cone		
blueberry	pentagon	square	rectangle	donut	star	cylinder				
cactusfruit	pentagon	heart								
cantaloupe	triangle	square	donut	star	pentagon	cone	cylinder			
carambola	square	hexagon	triangle	rectangle	pentagon	donut	star	cone	cylinder	heart
cherry	triangle	hexagon	square	heart	pentagon	donut	cylinder	star		
clementine	triangle	square	pentagon	star	rectangle	donut	heart			
cocos	triangle	rectangle								
date	square	donut	triangle	rectangle	cylinder					
fig	square	triangle	heart	star	pentagon					
grapefruit	triangle	rectangle	hexagon	star	square	pentagon	triangle	heart	donut	
guava	rectangle	square	hexagon	triangle	pentagon	heart				
huckleberry	rectangle	square	donut	cone						
kaki	square	heart	star							
kiwi	square	triangle	rectangle	hexagon	donut	star	heart	cone	cylinder	
kumquats	triangle	hexagon	cylinder							
lemon	hexagon	triangle	pentagon	donut	star	heart				
lime	donut	square	pentagon	star	heart	cone				
lychee	triangle	rectangle	donut	star	hexagon	heart	pentagon			
mandarine	hexagon	rectangle	donut	pentagon	heart	star				
mango	square	hexagon	pentagon	cone	cylinder	heart				
mangostan	triangle	rectangle	donut							
melon	square	triangle	hexagon	rectangle	donut	cone				
mulberry	square	triangle	hexagon	donut	rectangle	heart	star	cylinder		
orange	square	hexagon	donut	heart	pentagon					
papaya	rectangle	triangle	hexagon	square	pentagon	donut	star			
passionfruit	triangle	donut	star	heart						
peach	hexagon	donut	star	rectangle	square	pentagon	heart			
pear	pentagon	heart	donut							
physalis	donut	star								
pineapple	heart	star	donut							
pitahaya	triangle	square	pentagon	star						
plum	square	triangle	hexagon	donut	star	heart				
pomegranate	square	triangle	rectangle	hexagon	pentagon	donut	star	heart		
rambutan	square	rectangle	heart	donut						
raspberry	square	triangle	pentagon	star	donut	heart	hexagon	cone	cylinder	
salak	square	hexagon	rectangle	pentagon	donut	triangle	heart	cone	star	cylinder
strawberry	triangle	rectangle	square	donut	hexagon	pentagon	star	heart		
tangelo	triangle	hexagon	square	rectangle	pentagon	star	donut	cylinder	heart	
tomato	square	pentagon	star	rectangle						
watermelon	square	donut	rectangle	heart	star	cylinder				

strating consistent trends across various types of attribute modifications and object categories.

E.2. Investigating on Synthetic Original Data

To ensure a fair comparison, we also synthesize original objects using DALL-E [30]. Specifically, we generated images with the prompt “An image of {object}.” to evalu-

ate whether the use of generated images introduces performance degradation due to the generation model.

As shown in Tab. F, MLLMs’ performance on synthetic original data exhibits a slight drop of approximately 5 points in average accuracy, which is considerably smaller than the drop observed for attribute-modified objects. These results suggest that the use of generated images has minimal nega-

Table D. All animals and the modified colors for each animal in NEMO-extension.

Animal	Color ₁	Color ₂	Color ₃	Color ₄	Color ₅	Color ₆	Color ₇	Color ₈	Color ₉	Color ₁₀
blackbear	neon pink	iridescent blue	pure white	deep purple	emerald green	sky blue	golden			
bullfrog	bright yellow	neon pink	iridescent blue	pure white	fiery red	deep purple	sky blue	golden		
camel	vibrant green	neon pink	iridescent blue	pure white	deep purple	emerald green	sky blue			
cheetah	neon pink	iridescent blue	pure white	fiery red	deep purple	emerald green				
chimpanzee	neon pink	pure white	fiery red	deep purple	emerald green					
cobra	bright yellow	vibrant green	neon pink	iridescent blue	deep purple	emerald green	sky blue	golden		
coyote	vibrant green	pure white	fiery red	deep purple	sky blue	golden				
crocodile	vibrant green	neon pink	pure white	deep purple	emerald green					
deer	bright yellow	vibrant green	neon pink	pure white						
dolphin	bright yellow	vibrant green	pure white	emerald green						
duck	bright yellow	neon pink								
eagle	vibrant green	neon pink	deep purple	emerald green	golden					
elephant	bright yellow	vibrant green	neon pink	iridescent blue	pure white	fiery red	deep purple	emerald green	sky blue	golden
flamingo	bright yellow	deep purple	emerald green	sky blue	golden					
fox	bright yellow	neon pink	iridescent blue	deep purple	emerald green					
frog	bright yellow	neon pink	pure white							
giraffe	pure white	emerald green	golden							
goose	bright yellow	vibrant green	neon pink							
gorilla	bright yellow	neon pink								
grizzlybear	bright yellow	vibrant green	neon pink	iridescent blue	fiery red					
guineapig	bright yellow	vibrant green	neon pink	pure white	deep purple	fiery red				
hedgehog	vibrant green	neon pink	bright yellow	deep purple						
hippopotamus	pure white	emerald green	sky blue							
hummingbird	pure white	neon pink	deep purple	emerald green	golden	sky blue				
jaguar	vibrant green	iridescent blue	neon pink	pure white	deep purple	emerald green	sky blue			
kangaroo	neon pink	vibrant green	iridescent blue	fiery red	deep purple	emerald green	pure white			
koala	neon pink	bright yellow	fiery red	pure white	deep purple					
leopard	iridescent blue	fiery red	neon pink	sky blue	deep purple					
lion	vibrant green	neon pink	iridescent blue	pure white	fiery red	sky blue				
lizard	neon pink	pure white								
moose	vibrant green	neon pink	iridescent blue	pure white	emerald green	sky blue				
octopus	pure white	fiery red	deep purple	emerald green	sky blue	golden				
owl	bright yellow	vibrant green	neon pink	iridescent blue	pure white	fiery red	deep purple	emerald green	sky blue	
panda	neon pink	iridescent blue	deep purple							
peacock	neon pink	deep purple	sky blue	golden						
penguin	bright yellow	neon pink	pure white	fiery red	emerald green					
pig	fiery red	deep purple	golden							
porcupine	bright yellow	vibrant green	neon pink	iridescent blue	pure white					
raccoon	pure white	fiery red								
rhinoceros	vibrant green	neon pink	iridescent blue	deep purple	emerald green	golden				
seal	bright yellow	vibrant green	neon pink	fiery red	golden					
tiger	vibrant green	neon pink	fiery red	deep purple	emerald green					

tive impact on the performance of MLLMs, confirming that synthetic data from the generation model is a relatively reliable approach for evaluating their performance on attribute-modified objects.

E.3. Investigating on Other Question Prompts

Open questions using other prompts. In the main paper, we primarily used the prompt “*What is the object in this image? Please only reply with an object name.*” to evaluate the model’s performance in open questions. In this section, we experiment with alternative prompts, such as “*What is the fruit in this image? Please only reply with a fruit name.*”, which specifies the object category as fruit.

Open questions without limitation. We further examine the model’s performance with prompts like “*What is the object in this image?*” and “*What is the fruit in this image?*”,

allowing the model to provide responses of any length without restricting it to a single word.

As summarized in Tab. G, the experimental results reveal that variations in open question phrasing lead to marginal differences in accuracy. However, a noticeable performance drop persists on attribute-modified objects. These findings highlight the relative robustness of MLLMs to prompt phrasing variations within this evaluation context, while also emphasizing the challenges posed by attribute-modified objects.

F. More Discussion

F.1. Uniqueness of NEMO

NEMO is designed to evaluate MLLMs’ capabilities in object recognition, reasoning from commonsense to beyond it,

Table E. Performance in terms of accuracy (%) scores of 26 representative MLLMs on NEMO-extension, including open-sourced and commercial models, and random choice baseline. Higher score is better. The results cover original and shape-modified fruits, as well as original and color-modified animals. **Bold** marks the best results, and **original** marks the second best.

Method	Original Fruits				Shape-Modified Fruits				Original Animals				Color-Modified Animals			
	Open	Choice	Unsol.	Average	Open	Choice	Unsol.	Average	Open	Choice	Unsol.	Average	Open	Choice	Unsol.	Average
Baselines																
Random choice	-	24.5±2.2	26.4±2.0	25.5	-	25.5±2.4	25.2±2.1	25.4	-	25.1±3.0	23.5±2.1	24.3	-	25.1±3.3	25.6±2.5	25.4
Open-Sourced Models																
LLaVA-NeXT-8B [19]	42.5	64.3±0.6	19.9±13.5	42.2	28.5	57.6±0.6	27.2±16.4	37.8	57.8	82.5±1.4	33.7±11.6	58.0	58.3	73.6±1.3	40.6±18.7	57.5
LLaVA-NeXT-Qwen-32B [19]	59.5	83.4±0.8	39.2±12.2	60.7	49.6	81.8±0.8	43.5 ±15.3	58.3	57.8	93.2±0.6	37.5±10.5	62.8	57.3	83.0±0.9	47.6 ±14.5	62.6
LLaVA-NeXT-72B [19]	48.6	73.1±1.2	26.7±8.1	49.5	36.2	72.0±1.5	31.9±10.4	46.7	61.0	89.0±1.4	26.6±8.8	66.8	50.5	79.5±1.5	36.5±9.5	55.5
LLaVA-NeXT-110B [19]	53.5	76.5±1.3	8.3±3.5	46.1	35.0	75.8±1.4	14.5±4.1	41.8	60.1	87.2±0.7	12.5±4.0	53.3	55.5	76.5±1.9	13.3±4.9	48.4
InternVL2-1B [7]	45.3	66.2±2.0	13.1±7.2	41.5	30.4	67.6±2.0	21.4±7.9	39.8	56.9	81.0±1.5	18.7±6.2	52.2	46.3	75.4±1.8	12.2±4.4	44.6
InternVL2-2B [7]	49.9	67.1±0.4	14.2±0.8	43.7	37.3	56.6±1.3	8.6±1.3	34.2	57.8	80.3±0.7	14.6±2.1	50.9	57.3	74.1±1.0	7.7±0.7	46.4
InternVL2-4B [7]	52.3	71.0±0.9	15.2±5.2	46.2	35.0	71.0±3.1	15.8±4.3	40.6	65.1	88.5±0.6	8.2±1.2	53.9	58.7	76.8±1.5	6.4±0.6	47.3
InternVL2-8B [7]	52.2	85.0±0.4	31.6±5.0	56.3	34.2	67.7±0.8	30.0±7.1	44.0	60.6	88.8±1.0	31.0±3.5	60.1	60.6	81.1±0.9	29.1±5.6	57.3
InternVL2-26B [7]	77.7	95.4 ±0.7	25.7±8.3	66.3	63.8	86.2 ±0.7	21.4±5.8	57.1	71.1	91.5±1.1	15.8±2.5	59.5	68.8	83.8±1.6	18.8±3.1	57.1
InternVL2-40B [7]	68.1	94.7 ±0.5	43.8±8.8	68.9	51.2	86.3 ±1.5	41.8±6.5	59.8	64.2	91.8±0.5	32.4±8.3	62.8	62.8	84.3±1.0	34.0±10.0	60.4
InternVL2-LLaMA3-76B [7]	73.2	75.6±0.9	31.2±4.7	60.0	54.2	73.4±2.9	31.2±5.3	52.9	61.0	87.6±2.1	19.5±4.6	56.0	62.8	79.9±0.7	17.8±3.8	53.5
Cambrian-1-3B [34]	61.9	89.7±0.9	42.7±7.7	64.8	46.9	84.5±0.6	25.4±3.9	52.3	90.4	89.1±1.0	44.6 ±3.3	74.7	86.2	83.7±0.8	40.6±2.2	70.2
Cambrian-1-8B [34]	66.3	87.3±1.1	63.0 ±7.1	72.2	57.7	84.3±0.8	45.3 ±3.9	62.4	93.6	94.4 ±0.8	49.3 ±4.5	79.1	82.6	86.7 ±1.1	48.3 ±1.5	72.5
Cambrian-1-13B [34]	62.8	85.7±0.3	44.6±6.5	64.4	61.5	81.6±0.8	34.1±2.6	59.1	92.7	93.6 ±1.8	40.1±4.0	75.5	77.1	86.5±2.8	39.8±2.5	67.8
Cambrian-1-34B [34]	69.5	91.3±1.3	57.0 ±2.3	72.6	56.2	86.0±1.2	33.8±3.8	58.7	94.5	91.6±1.4	44.4±4.3	76.8	86.2	84.5±1.1	40.3±3.3	70.3
Yi-VL-6B [41]	54.1	87.8±1.0	42.5±8.0	61.5	40.4	79.9±2.1	37.9±10.0	52.7	61.0	81.3±1.2	37.4±8.6	59.9	59.2	73.5±0.8	34.3±11.0	55.7
Yi-VL-34B [41]	54.0	90.7±1.2	26.5±9.4	57.1	36.9	74.4±1.2	27.1±7.7	46.1	67.0	83.5±1.0	21.3±12.5	57.3	57.3	79.6±1.5	37.1±12.4	58.0
InstructBLIP-7B [9]	58.7	43.0±10.9	5.8±4.3	35.8	46.5	48.5±10.1	14.4±18.0	36.5	69.7	58.6±56.3	12.8±10.6	47.0	63.8	54.0±8.7	13.9±8.7	43.9
InstructBLIP-13B [9]	57.8	56.0±11.6	5.8±6.0	39.9	38.8	57.0±11.2	37.8±33.3	44.5	65.6	69.2±11.1	35.1±37.1	56.6	61.0	64.1±8.6	39.2±35.3	54.8
MiniGPT4-7B [49]	56.4	59.1±1.7	35.9±3.7	50.5	44.2	30.0±5.4	7.2±3.5	27.1	83.9	68.1±1.1	6.4±1.2	52.8	75.2	48.3±2.1	7.3±2.3	43.6
MiniGPT4-13B [49]	56.4	58.9±2.9	39.9±0.9	51.7	44.6	45.3±0.9	7.1±3.5	32.3	89.4	76.6±1.3	5.0±2.8	57.0	72.9	65.9±1.1	6.0±2.6	48.3
MiniGPT4-v2-7B [6]	55.5	58.7±4.5	30.1±20.4	48.1	35.4	49.9±4.9	17.4±25.6	34.2	69.7	74.6±3.5	6.0±8.8	50.1	61.5	68.8±3.6	9.0±15.2	46.4
Commercial Models																
GPT-4o [28]	88.1	93.3 ±0.4	78.8 ±3.4	86.7	61.5	88.7±0.3	86.2±6.4	78.8	78.4	97.9 ±0.5	82.4 ±2.7	86.2	71.1	90.8 ±0.7	82.1 ±7.0	81.3
GPT-4o-mini [28]	79.1	88.0±0.1	78.0 ±1.9	81.7	61.5	85.6±1.1	82.2 ±3.1	76.4	79.4	97.4 ±0.5	82.5 ±1.7	86.4	70.6	87.9±0.8	84.5 ±3.7	81.0
Gemini-1.5-Flash [14]	86.6	92.9±0.1	63.7±3.4	81.1	71.2	89.6 ±1.1	43.8±15.5	68.2	75.7	95.0±1.2	22.3±7.3	64.3	70.2	89.9±1.1	24.8±8.1	61.6
Gemini-1.5-Pro [14]	84.9	94.7 ±0.6	56.0±10.7	78.5	77.3	94.1 ±0.9	58.8±8.0	76.7	79.8	96.8±0.6	30.3±14.6	68.9	72.9	92.4 ±2.2	26.5±10.9	63.9

Table F. Performance in terms of accuracy (%) scores of representative MLLMs on original objects from NEMO and synthetic original objects. Higher score is better. **Bold** marks the best results, and **original** marks the second best.

Method	Original Objects				Synthetic Original Objects			
	Open	Choice	Unsol.	Average	Open	Choice	Unsol.	Average
Open-Sourced Models								
LLaVA-NeXT-8B [19]	42.0	77.2±0.8	27.1±13.9	48.8	41.6	64.9±0.7	21.0±14.0	42.5
LLaVA-NeXT-Qwen-32B [19]	58.0	93.8±0.3	42.0 ±16.5	64.6	56.0	84.6±0.7	39.9 ±12.8	60.2
LLaVA-NeXT-72B [19]	47.6	84.5±0.5	28.2±9.7	53.4	45.1	73.6±1.3	30.0±8.3	49.6
LLaVA-NeXT-110B [19]	51.3	85.5±1.2	16.2±8.3	51.0	47.8	77.7±1.0	9.6±5.0	45.0
InternVL2-1B [7]	45.3	71.5±1.0	21.6±10.4	46.1	42.2	64.7±1.6	14.3±7.7	40.4
InternVL2-2B [7]	49.6	68.4±0.5	13.8±0.4	43.9	46.4	65.8±1.5	25.0±25.4	45.7
InternVL2-4B [7]	50.9	82.9±0.7	18.6±6.0	50.8	42.9	70.9±0.9	16.8±5.0	43.5
InternVL2-8B [7]	50.7	84.3±0.5	31.3±5.2	55.4	44.2	73.7±0.8	28.1±6.9	48.7
InternVL2-26B [7]	79.3	96.0 ±0.5	24.3±8.1	66.5	74.4	87.9 ±1.6	23.8±5.6	62.0
InternVL2-40B [7]	69.6	95.4 ±0.3	44.9 ±8.6	70.0	65.1	92.3 ±1.4	53.3 ±8.6	70.2
InternVL2-LLaMA3-76B [7]	73.3	87.0±0.9	35.7±6.1	65.3	64.7	78.0±0.9	33.4±5.4	58.8
Commercial Models								
GPT-4o [28]	90.9	99.3 ±0.2	84.2 ±1.9	91.5	86.2	93.8 ±0.3	79.4 ±2.9	86.5
GPT-4o-mini [28]	85.3	95.4±0.4	87.0 ±1.1	89.2	81.3	88.8±0.1	79.9 ±1.7	83.3
Gemini-1.5-Flash [14]	86.2	96.1±1.2	57.9±15.0	80.1	87.6	93.7±0.1	66.2±3.2	82.5
Gemini-1.5-Pro [14]	86.4	99.2 ±0.4	68.3±1.0	84.6	85.1	94.9 ±0.5	58.0±10.7	79.3

by introducing attribute-modified objects alongside original ones. This new benchmark is unique for two main reasons:

Reasoning from commonsense to beyond commonsense. NEMO bridges commonsense recognition with beyond-commonsense reasoning by incorporating both original and attribute-modified objects. It evaluates the model’s transi-

tion from recognizing original objects to understanding uncommon, modified variations, reflecting a more comprehensive and nuanced measure of MLLMs’ flexibility.

Multi-question designing. NEMO employs a well-constructed question design with three distinct question types: open questions, multiple-choice questions, and un-

Table G. Performance in terms of accuracy (%) scores of representative MLLMs on NEMO. Higher score is better. The evaluation spans original and synthetic original objects across four open question types: open questions requiring an object name as the response (Obj. Nam.); open questions requiring a fruit name as the response (Fru. Nam.); open questions with unrestricted object responses of any length (Obj. Unre.), and (4) open questions with unrestricted fruit responses of any length (Fru. Unre.). **Bold** marks the best results, and **original** marks the second best.

Method	Original Objects				Attribute-Modified Objects			
	Obj. Nam.	Fru. Nam.	Obj. Unre.	Fru. Unre.	Obj. Nam.	Fru. Nam.	Obj. Unre.	Fru. Unre.
Open-Sourced Models								
LLaVA-NeXT-8B [19]	42.0	54.0	58.7	59.3	24.9	34.2	26.7	32.2
LLaVA-NeXT-Qwen-32B [19]	58.0	66.9	61.1	75.8	35.8	47.3	43.1	52.9
LLaVA-NeXT-72B [19]	47.6	50.9	48.9	59.8	24.2	26.9	23.3	26.7
LLaVA-NeXT-110B [19]	51.3	52.9	55.6	53.6	26.9	30.0	24.0	28.4
InternVL2-1B [7]	45.3	43.1	38.7	40.4	24.0	29.3	19.8	22.4
InternVL2-2B [7]	49.6	51.3	52.9	54.7	25.6	30.0	22.9	27.3
InternVL2-4B [7]	50.9	48.7	44.2	50.9	23.3	28.9	19.6	23.8
InternVL2-8B [7]	50.7	56.7	57.6	61.6	25.8	28.7	23.8	31.3
InternVL2-26B [7]	79.3	75.6	75.3	81.6	53.3	56.9	49.1	54.0
InternVL2-LLaMA3-76B [7]	73.3	75.6	79.8	80.2	44.4	50.0	42.2	46.9
Commercial Models								
GPT-4o [28]	90.9	92.4	87.8	92.0	56.2	62.0	47.8	58.7
GPT-4o-mini [28]	85.3	88.4	86.0	91.8	49.6	59.1	43.8	54.4
Gemini-1.5-Flash [14]	86.2	92.0	88.0	91.1	63.3	69.1	56.2	63.1
Gemini-1.5-Pro [14]	86.4	88.9	89.1	92.7	62.2	67.3	56.0	63.3

Q: What is the object in this image? Please only reply with an object name.

Correct Answer: guava

GPT-4o: **pumpkin**

GPT-4o-mini: **pumpkin**

Gemini-1.5-Flash: **fruit**

Gemini-1.5-Pro: guava

LLaVA-NeXT-8B: **pumpkin**

LLaVA-NeXT-Qwen-32B: **brain**

LLaVA-NeXT-72B: **pumpkin**

LLaVA-NeXT-110B: **pumpkin**

InternVL2-1B: **potato**

InternVL2-2B: **pumpkin**

InternVL2-4B: **apple**

InternVL2-8B: **pumpkin**

InternVL2-26B: **pumpkin**

InternVL2-40B: **pomegranate**

InternVL2-LLaMA3-76B: **melon**

Yi-VL-6B: **brain**

Yi-VL-34B: **brain**

InstructBLIP-7B: The object in this image is a **grapefruit**.

InstructBLIP-13B: **pear**

MiniGPT4-7B: The object in this image is a purple **grapegrenade**.

MiniGPT4-13B: The object in this image is a **grape**.

MiniGPT-v2-7B: **plum**

Cambrian-1-3B: The object in this image is a fruit, specifically a **pear**.

Cambrian-1-8B: The object in the image is a fruit, specifically designed to resemble a brain. It is not a real fruit but rather a creative representation, likely intended for artistic or illustrative purposes. The name of the object, based on its visual characteristics, would be "**brain-shaped fruit**."

Cambrian-1-13B: The object in the image is a fruit that has been artistically altered to resemble a human brain. It is not a natural fruit but rather a creative representation, possibly intended for artistic or conceptual purposes. The object's name, based on its visual characteristics, would be "**brain-shaped fruit**."

Cambrian-1-34B: The object in this image is a **pumpkin**.



A rich purple guava.

Figure D. Failures responses from 26 MLLMs for the open question on a attribute-modified sample of "A rich purple guava" in NEMO.

solvable questions. This setup assesses the model's ability to identify objects, differentiate between correct and distractor options, and recognize when no correct answer is available, offering a comprehensive evaluation of the

Q: What is the object in this image? Please only reply with an object name.

Correct Answer: kumquats

GPT-4o: **tomato**

GPT-4o-mini: **tomatoes**

Gemini-1.5-Flash: kumquats

Gemini-1.5-Pro: **olives**

LLaVA-NeXT-8B: **tomato**

LLaVA-NeXT-Qwen-32B: **tomato**

LLaVA-NeXT-72B: **oranges**

LLaVA-NeXT-110B: kumquats

InternVL2-1B: **red apples**

InternVL2-2B: **pomegranate**

InternVL2-4B: **pomegranate**

InternVL2-8B: **fruit**

InternVL2-26B: kumquats

InternVL2-40B: **fruit**

InternVL2-LLaMA3-76B: **fruit**

Yi-VL-6B: **tomatoes**

Yi-VL-34B: **tomatoes**

InstructBLIP-7B: The object in this image is **tomatoes**.

InstructBLIP-13B: **tomato**

MiniGPT4-7B: The object in this image is a square box filled with **red tomatoes**.

MiniGPT4-13B: The object in the image is a box of **tomatoes**.

MiniGPT-v2-7B: The object in the image is a white box containing a group of **red strawberries**.

Cambrian-1-3B: The object in this image is a box of **tomatoes**.

Cambrian-1-8B: The object in the image is a box of **tomatoes**.

Cambrian-1-13B: The object in this image is a box of **cherry tomatoes**. Cherry tomatoes are a type of tomato that is smaller and sweeter than regular tomatoes, often used in salads, as a garnish, or eaten fresh. The box is designed to hold the tomatoes securely and is likely made of a sturdy material to protect the delicate fruit inside.

Cambrian-1-34B: The object in this image is a collection of **tomatoes**.



Deep red kumquats.

Figure E. Failures responses from 26 MLLMs for the open question on a attribute-modified sample of "deep red kumquats" in NEMO.

model's strengths and limitations.

Q: What is the object in this image? Please only reply with an object name.

Correct Answer: mandarine

GPT-4o: **apple**

GPT-4o-mini: **oranges**

Gemini-1.5-Flash: **fruit**

Gemini-1.5-Pro: **tangerine**

LLaVA-NeXT-8B: **oranges**

LLaVA-NeXT-Qwen-32B: **apple**

LLaVA-NeXT-72B: **grape**

LLaVA-NeXT-110B: **fruit**

InternVL2-1B: **red apples**

InternVL2-2B: **apple**

InternVL2-4B: **apple**

InternVL2-8B: **apple**

InternVL2-26B: **grapefruit**

InternVL2-40B: **oranges**

InternVL2-LLaMA3-76B: **apple**

Yi-VL-6B: **apple**

Yi-VL-34B: **apple**

InstructBLIP-7B: The object in this image is a **fruit**.

InstructBLIP-13B: **apple**

MiniGPT4-7B: The object in this image is a group of **pink apples**.

MiniGPT4-13B: **6 pink apples** arranged in a circle on a white surface.

MiniGPT-v2-7B: **fruit**

Cambrian-1-3B: The object in this image is a fruit, specifically a citrus fruit, which appears to be a **tangerine** or a similar variety. This identification is based on the characteristic bright red color, the size and shape of the fruit, and the presence of a stem and a small indentation at the top, which are typical features of citrus fruits.

Cambrian-1-8B: The object in this image is a collection of **persimmons**. Persimmons are a type of fruit known for their sweet, honey-like flavor and smooth, glossy skin. They are often eaten fresh, dried, or used in cooking and baking. The bright red color of the persimmons in the image is characteristic of the sweet variety, which is typically eaten raw.

Cambrian-1-13B: The object in this image is a collection of stylized fruits, specifically designed to resemble citrus fruits such as **oranges or tangerines**. The uniformity in color and the presence of the stem suggest that they are intended to be a representation of real fruit, but the exaggerated size and the smooth, untextured surface indicate that they are likely not actual edible fruit but rather artistic renderings or models.

Cambrian-1-34B: The object in this image is a plate of **kumquats**.



Vivid pink mandarines.

Figure F. Failures responses from 26 MLLMs for the open question on a attribute-modified sample of “*vivid pink mandarines*” in NEMO.

F.2. Is NEMO easy?

Yes, NEMO is easy for humans. As demonstrated by the results in the main paper Sec. 5.1, humans can readily identify attribute-modified objects using their prior knowledge. However, through our experiments, we find NEMO poses significant challenges for current MLLMs due to the following reasons:

From the model perspective. On the one hand, the full generalization capabilities of vision encoders are not fully realized in current MLLMs. On the other hand, larger LLMs often degrade the effectiveness of vision encoders during fine-tuning, leading to suboptimal integration.

From the data perspective. Spurious correlations between visual features hinder MLLMs’ ability to accurately understand attribute-modified objects in NEMO.

Therefore, our NEMO can serve as as a testbed to lay out potential roadmaps to enhance versatile and resilient MLLMs.



Figure H. Sample for each shape-modified object in NEMO-extension.



Figure I. Sample for each original animal in NEMO-extension.

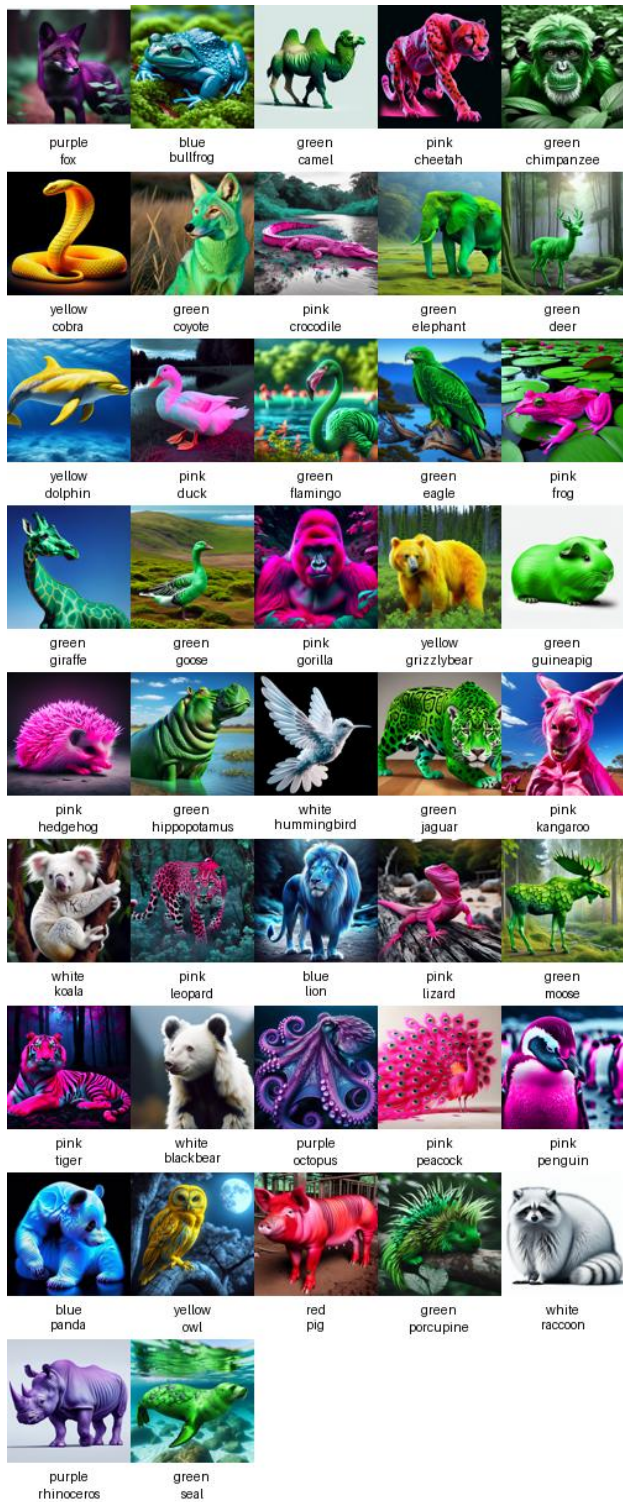


Figure J. Sample for each color-modified animal in NEMO-extension.